

# Utilization of synchrotron radiation: current status and prospects

G. N. Kulipanov and A. N. Skrinskiĭ

*Nuclear Physics Institute, Siberian Division, USSR Academy of Sciences, Novosibirsk  
Usp. Fiz. Nauk 122, 369-418 (July 1977)*

The review discusses the research and technological potential of contemporary sources of synchrotron radiation. A comparison is made of various sources of ultraviolet and x radiation. Characteristics are given of present electron storage rings—the principal sources of synchrotron radiation, and the means and limits of their further refinement are discussed. The features of performing experiments with synchrotron radiation in storage rings are considered. The main formulas characterizing the properties of synchrotron radiation are presented in a form convenient for practical calculations. The regions of application of synchrotron radiation are discussed (x-ray microscopy, x-ray structural analysis, and molecular, atomic, and nuclear spectroscopy). The principal attention is given to those questions in which the use of synchrotron radiation opens new possibilities. The prospects for practical application of synchrotron radiation are discussed (metrology, medicine, materials science, radiation technology).

PACS numbers: 41.70.+t, 29.20.Dh

## CONTENTS

1. Introduction . . . . .	559
2. Basic Properties of Synchrotron Radiation . . . . .	560
3. Possibilities of Electron Storage Rings—the Principal Sources of Synchrotron Radiation . . . . .	564
4. Use of Synchrotron Radiation for X-Ray Microscopy . . . . .	569
5. Use of Synchrotron Radiation for X-Ray Structure Analysis . . . . .	575
6. Study of Interaction of Radiation with Atoms, Molecules, and Condensed Matter . . . . .	578
7. Use of Synchrotron Radiation to Determine the Chemical Composition of Objects . . . . .	579
8. Nuclear Spectroscopy and Related Questions . . . . .	580
9. Prospective Applications of Synchrotron Radiation . . . . .	582
10. Conclusion . . . . .	584
Appendix . . . . .	584
References . . . . .	585

## 1. INTRODUCTION

The synchrotron radiation (SR) or magnetic bremsstrahlung arising on motion of high-energy charged particles (electrons and positrons) in a magnetic field has already been used long and fruitfully in high energy physics. It is very convenient to measure the characteristics of beams in accelerators and storage rings by means of synchrotron radiation. Here the sensitivity of the method is the highest achievable—the radiation of a single electron or positron in a storage ring is easily observed. The use of the radiation damping produced by synchrotron radiation is very important; it permits compression of beams to very small dimensions and repeated storage of new groups of particles, which is fundamental in obtaining intense positron beams. Synchrotron radiation leads to appearance of polarization of the electrons and positrons moving in a storage ring, which permits intense polarized beams of electrons and positrons to be obtained (including colliding beams).

Use of synchrotron radiation is beginning for identification of high energy electrons (~100 GeV) and for sep-

aration of them from the general flux of high energy secondary particles obtained in large proton accelerators. Detection of the synchrotron radiation of fast electrons in the fields of astronomical objects permits important information to be obtained on these formations.

In recent years synchrotron radiation has been more and more widely used in various experiments where intense fluxes of vacuum ultraviolet and x radiation are required. Interest in synchrotron radiation on the part of physicists with various specialties, biologists, and chemists rose especially sharply after the construction of electron storage rings of high energy (of the order of 1 GeV and higher) for experiments with colliding electron-positron beams. The usable intensity of synchrotron radiation of already existing storage rings is many orders greater than that of any other sources in the range of wavelengths from 1000 Å to 0.1 Å (range of photon energy from 10 eV to 100 keV). In the near future it will be possible to increase the intensity of synchrotron radiation by many times and to increase the energies of the photons generated.

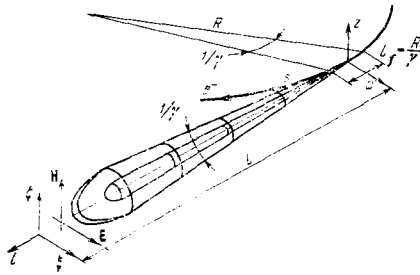


FIG. 1. Synchrotron radiation—geometrical arrangement and designations.

The development of the theory of synchrotron radiation was stimulated by the study of various atom models, [1] by cosmic-ray physics, [2] and by creation of charged-particle accelerators. [3,4] Detailed studies of the theory of synchrotron radiation (total intensity, angular and spectral distribution, polarization properties) were carried out in Refs. 5–8. At the present time the theory of synchrotron radiation is highly developed and is rather completely described in textbooks. [9–12]

The detailed experimental study of the properties of synchrotron radiation was carried out in the fifties and sixties and has been described in reviews. [13,14]

The applications of synchrotron radiation have already been discussed in several books and reviews. [15–18]. Our purpose is to provide a “user’s guide” to the present possibilities of SR sources and to discuss the means and limits of their further development. In addition we shall discuss the main fields of application of this class of radiation sources.

In every case the principal attention will be devoted to those questions in which application of SR opens fundamentally new possibilities. Our discussion of these problems will unavoidably be fragmentary. It will strive to interest the broadest possible group of synchrotron radiation users and to stimulate them to go over to practical work in this area. The sooner and more actively the interested persons begin to do this, the greater the chances of success for the rapidly developing national programs on use of SR in other countries. At the present time there is a real possibility of being at the frontier of a field which can have revolutionary significance for many branches of science and technology.

## 2. BASIC PROPERTIES OF SYNCHROTRON RADIATION

### A. Qualitative characteristics of synchrotron radiation of one electron

We shall discuss the radiation of an ultrarelativistic electron ( $\gamma = E/mc^2 \gg 1$ , and in the case of interest even  $\gamma > 100$ , where  $E$  is the electron energy and  $mc^2 \approx 0.5$  MeV is its rest energy) moving in some magnetic field (a complex configuration) near a closed trajectory. Just this situation is characteristic of the cyclic accelerators and storage rings of interest to us.

Let the electron trajectory be close to a circle of

radius  $R$  (Fig. 1) over a sufficiently great length. Then the radiation will be concentrated near the orbit plane (the principal power is concentrated in an angle of the order  $\psi_{x,s} \sim 1/\gamma$ ). The radiation reaches a point of observation located in this plane along a tangent drawn to the trajectory from this point. The length of the portion of the trajectory providing the main contribution to the radiation power at the chosen observation point—the radiation formation length—will be of the order

$$L_f \approx \frac{R}{\gamma} = \frac{mc^2}{eH},$$

where  $e$  is the electronic charge and  $H$  is the magnetic field at the point of radiation.

The electromagnetic wave radiated by an electron on repeated passage will arrive at the point of observation in the form of a burst of electric and magnetic field, the length of the burst being of the order

$$l_{\text{burst}} \approx \frac{R}{\gamma^3} = \frac{mc^2}{\gamma^2 eH}.$$

Accordingly the radiation spectrum will have a maximum at a wavelength

$$\lambda_c \sim \frac{R}{\gamma^3}.$$

We note that the angular divergence of the radiation  $\psi \sim 1/\gamma$  at a wavelength  $\lambda \sim R/\gamma^3$  corresponds to an “effective” transverse dimension of the source equal in order of magnitude to

$$\Delta_{\perp} \sim \Delta_{\parallel} \sim \frac{R}{\gamma^2}.$$

The electric and magnetic field at the maximum of the burst will be

$$E_{\text{max}} \approx \frac{4\gamma^3 e}{RL},$$

where  $L$  is the distance from the point of observation to the point of radiation. Correspondingly, the energy density of the radiation flux from a single electron in periodic motion, estimated as the average over time of  $cE^2/4\pi$  ( $c$  is the velocity of light), will be

$$I_1 \approx \frac{e^4}{m^2 c^3} \frac{H^2 \gamma^3}{L^2}.$$

The energy flux density  $I_1$  determines the illumination of a sample at a distance  $L$  from the point of radiation.

The total intensity of radiation in all directions is

$$P_1 = I_1 S \approx \frac{e^4 H^2}{m^2 c^3} \gamma^2,$$

where  $S = 4\pi L^2/\gamma$  is the total area of the regions eliminated by normal incidence synchrotron radiation and located at a distance  $L$  from the point of radiation.

Another important characteristic is the quantity which determines the energy loss of an electron per revolu-

tion. If the magnetic field in the regions of radiation is constant, the energy loss per revolution is

$$W_{\text{rev}} = \frac{4\pi e^4 H^2 \gamma^2}{3m^2 c^4} R = \frac{4\pi e^2}{3R} \gamma^4.$$

The total number of photons of all energies radiated by one electron per revolution is

$$N_{1\Sigma} \approx \frac{W_{\text{rev}}}{hc} \approx \frac{2\pi e^2}{hc} \gamma = 2\pi\alpha\gamma.$$

where  $\hbar$  is Planck's constant and  $\alpha \approx 1/137$  is the fine-structure constant.

For a single passage of the electron, the radiation spectrum at the point of observation will naturally be complicated. For the wavelength region of interest to us,  $\lambda \ll R$ , the successive traversals of an electron in practical situations are uncorrelated and the spectrum in this region of wavelengths for "periodic" motion of the radiating electron remains complex. The intensity of radiation in the long-wavelength part of the spectrum for  $\lambda > \lambda_c$  falls off slowly as  $(\lambda_c/\lambda)^{1/3}$ , and in the short-wavelength part of the spectrum for  $\lambda < \lambda_c$  a rapid exponential drop is observed  $\sim \sqrt{\lambda_c/\lambda} \exp\{-\lambda_c/\lambda\}$ .

It should be noted that the angular divergence of radiation with  $\lambda_1 > \lambda_c$  is determined by the value of the energy at which the radiation spectrum has a maximum for this wavelength,  $\psi_{\lambda_1} \sim 1/\gamma_1$ , where  $\gamma_1 = (R/\lambda_1)^{1/3}$ , and therefore  $\psi_\lambda \sim (\lambda/R)^{1/3}$ .

The range of angles with which the radiation from one electron arrives at the point of observation, after averaging over time, can be characterized by introduction of an "effective" radial dimension equal to

$$\Delta_{1r} \sim R\psi_\lambda^2.$$

In the vertical direction the situation is more complicated: If the point of observation is in the orbit plane, the interval of angles of arrival of radiation at the point of observation is zero; with departure from this plane the interval rises linearly and corresponds to a vertical dimension

$$\Delta_{1z} \sim R\psi_\lambda \frac{\xi}{L},$$

where  $\xi$  is the deviation from the orbit plane,  $L$  is the distance from the point of radiation to the point of observation, and  $\psi_\lambda$  is the angular divergence of SR at wavelength  $\lambda$ . Since the principal power is radiated at a vertex angle  $\xi/L = \psi_\lambda$ , the "effective" vertical dimension turns out also to be equal to  $R\psi_\lambda^2$ .

The electric field intensity vector at a point of observation lying in the orbit plane (see Fig. 1) is perpendicular to the tangent drawn from the point of observation to the electron trajectory and lies in the orbit plane; the magnetic field of the wave is perpendicular to this plane, i. e., the radiation in the orbit plane is linearly polarized. If the point of observation is outside the orbit plane, the radiation becomes elliptically polarized.

The direction of rotation of the radiation field vector coincides with the electron rotation direction seen from the point of observation. Therefore on different sides of the orbit plane the radiation has left and right elliptical polarization.

If  $N$  electrons are moving in the storage ring, then, regardless of their grouping in bunches, for the short-wavelength radiation of interest to us the relative positions of the electrons can be considered uncorrelated. In this case the radiation is incoherent and the energy fluxes of individual electrons simply add, i. e.,  $I_N = NI_1$ .

The magnetic field in the radiation region may not be constant along the trajectory. An extremely efficient means of increasing the intensity of SR is placement in a portion of the storage ring orbit of magnetic wigglers which produce a periodic magnetic field of alternating sign with a spatial period  $2d$ . Here a wavelength  $\sim d/\gamma^2$  is emphasized in the radiation spectrum. Regardless of the wiggler parameters (magnetic field strength, period  $2d$ , wiggler length  $L_{w1}$ ) and electron energy, the total energy loss in the wiggler is

$$P_{\Sigma w1} \sim E^2 \overline{H^2} L_{w1}$$

The spectral and angular distributions of the synchrotron radiation depend on the wiggler parameters.<sup>[19,20]</sup>

1) If the radiation formation length  $L_f = R\varphi_\lambda$  is much less than  $d$ , then the characteristics of the SR from a given portion of the trajectory are determined by the local curvature of the trajectory. The wavelength  $d/\gamma^2$  falls in the nondominant part of the radiation spectrum. Here the characteristics of the SR flux at the point of observation are obtained as the result of summation of fluxes from different portions of the trajectory.

2) In the so-called undulator regime, when  $d < R\psi_\lambda = (\gamma mc^2/eH)\psi_\lambda \approx mc^2/eH$ , the required magnetic field for a sinusoidal variation of the magnetic field along the trajectory need be no more than thousands of oersteds ( $dH \leq 5300 \text{ Oe-cm}$ ). Here the total radiant power ( $P_\Sigma \sim H^2$ ) drops, but in the radiation spectrum at zero angle the wavelength  $\lambda_{\text{und}} \sim d/\gamma^2$  is emphasized with a relative line width proportional to the reciprocal number of periods in the undulator. The undulator regime permits removal of the short-wavelength part of the radiation and permits radiation with complete linear or circular polarization to be obtained by use of an undulator with a transverse field of alternating sign or a field which rotates along the trajectory.

## B. Quantitative information on the properties of synchrotron radiation

In this section we shall present in a form convenient for practical calculations the basic formulas characterizing the properties of synchrotron radiation of electrons moving in some portion of a circular orbit with radius  $R(m)$ . In the formulas we used the following parameters of the storage ring:  $E(\text{GeV})$ —the particle energy;  $I(A)$  =  $1.6 \times 10^{-19} N_e f_0 (c^{-1})$ —the current in the storage ring ( $N_e$  is the number of particles,  $f_0$  is the frequency of revolution);  $H(\text{kOe})$ ,  $R(m) = (100/3) E(\text{GeV})/H(\text{kOe})$ —the

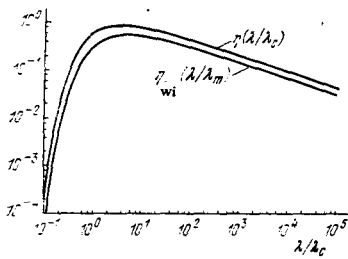


FIG. 2. Universal function  $\eta(\lambda/\lambda_c)$  determining the spectral characteristics of synchrotron radiation as a function of the parameter  $\lambda/\lambda_c$ .

magnetic field and radius of curvature of the trajectory at the point of radiation; and  $L(m)$ —the distance from the point of radiation to the point of observation.

1) *Illumination*—the power of a beam of synchrotron radiation summed over all wavelengths, reaching an area  $1 \text{ mm}^2$  located in the orbit plane at a distance  $L$  from the point of radiation:

$$I_C (\text{W/mm}^2) = 14 \frac{E^5 (\text{GeV}) I (\text{A})}{R (\text{m}) L^2 (\text{m})} \\ = 0.42 \frac{H (\text{kOe}) E^4 (\text{GeV}) I (\text{A})}{L^2 (\text{m})}.$$

2) *The power of the SR beam*—the synchrotron radiation power summed over all wavelengths, integrated over the vertical angle, per milliradian of radial angle,

$$P_C (\text{W/mrad}) = \frac{14 E^4 (\text{GeV}) I (\text{A})}{R (\text{m})} \\ = 0.42 H (\text{kOe}) E^3 (\text{GeV}) I (\text{A}).$$

3) *Photon flux*—total number of photons of all energies radiated by electrons per milliradian of radial angle:

$$\dot{N}_C (\text{photons/sec-mrad}) = 1.3 \cdot 10^{17} E (\text{GeV}) I (\text{A}).$$

4) *Spectral illumination*—the illumination at a given wavelength in a wavelength interval  $\Delta\lambda/\lambda$ :

$$I_\lambda (\text{W/mm}^2) = 59 \frac{E^2 (\text{GeV}) I (\text{A})}{\lambda (\text{\AA}) L^2 (\text{m})} \eta\left(\frac{\lambda}{\lambda_c}\right) \nu^{-1}\left(\frac{\lambda}{\lambda_c}\right) \frac{\Delta\lambda}{\lambda},$$

where

$$\lambda_c (\text{\AA}) = \frac{5.59 R (\text{m})}{E^3 (\text{GeV})} = \frac{186}{H (\text{kOe}) E^2 (\text{GeV})}, \quad 1)$$

$\eta(\lambda/\lambda_c)$  is a universal spectral function, a plot of which is shown in Fig. 2, and  $\nu(\lambda/\lambda_c)$  is a universal angular function, a plot of which is shown in Fig. 3 (see the angular distribution).

5) *Spectral power*—the power of an SR beam at a given wavelength in a wavelength interval  $\Delta\lambda/\lambda$ :

<sup>1)</sup>It should be noted that in Refs. 10 and 12, in contrast to the generally accepted value, other definitions of  $\lambda_c$  are used:  $\lambda_c = \lambda_c/2$  in Ref. 10,  $\lambda_c = 3\lambda_c/4$  in Ref. 12.

$$P_\lambda (\text{W/mrad}) = 48.6 \frac{I (\text{A}) E (\text{GeV})}{\lambda (\text{\AA})} \eta\left(\frac{\lambda}{\lambda_c}\right) \frac{\Delta\lambda}{\lambda} = 0.62 \frac{P_C}{\lambda/\lambda_c} \eta\left(\frac{\lambda}{\lambda_c}\right) \frac{\Delta\lambda}{\lambda}.$$

6) *Spectral photon flux*—the flux of photons at a given wavelength  $\lambda$  in a wavelength interval  $\Delta\lambda/\lambda$ :

$$\dot{N} (\lambda) (\text{photons/sec-mrad}) \\ = 2.46 \cdot 10^{16} I (\text{A}) E (\text{GeV}) \left(\frac{\lambda}{\lambda_c}\right) \frac{\Delta\lambda}{\lambda} = 0.19 \dot{N}_C \eta\left(\frac{\lambda}{\lambda_c}\right) \frac{\Delta\lambda}{\lambda}.$$

For  $\lambda/\lambda_c \gg 1$  and  $\lambda/\lambda_c \ll 1$  we can use the simple formulas:

$$\dot{N} (\lambda) (\text{photons/sec-mrad}) \approx 9.35 \cdot 10^{16} I (\text{A}) \left(\frac{R (\text{m})}{\lambda (\text{\AA})}\right)^{1/3} \frac{\Delta\lambda}{\lambda} \quad \left(\frac{\lambda}{\lambda_c} \gg 1\right),$$

$$\dot{N} (\lambda) (\text{photons/sec-mrad}) \\ = 3.08 \cdot 10^{16} I (\text{A}) E (\text{GeV}) \sqrt{\frac{\lambda_c}{\lambda}} \exp\left(-\frac{\lambda_c}{\lambda}\right) \frac{\Delta\lambda}{\lambda} \quad \left(\frac{\lambda}{\lambda_c} \ll 1\right).$$

7) *Angular distribution*. The width of the angular distribution of radiation with  $\lambda \sim \lambda_c$  (the angle at which the intensity of radiation decreases by a factor of two in comparison with the intensity in the orbital plane) is

$$\Psi_{\lambda_c} (\text{mrad}) = \frac{0.82}{E (\text{GeV})} \quad (\lambda = \lambda_c).$$

For  $\lambda \gg \lambda_c$  this angle is greater than  $\Psi_{\lambda_c}$ , it does not depend on the electron energy, and it is determined only by the wavelength and the radius of curvature at the point of radiation,

$$\Psi_\lambda (\text{mrad}) = 0.66 \left(\frac{\lambda (\text{\AA})}{R (\text{m})}\right)^{1/3} \quad (\lambda \gg \lambda_c).$$

In the case when  $\lambda \ll \lambda_c$ , the width of the angular distribution is less than  $\Psi_{\lambda_c}$ , and it is determined only by the wavelength and by the magnetic field at the point of radiation,

$$\Psi_\lambda (\text{mrad}) = 5 \cdot 10^{-2} \sqrt{\lambda (\text{\AA}) H (\text{kOe})} \quad (\lambda \ll \lambda_c).$$

The ratio  $\Psi_\lambda/\Psi_{\lambda_c}$  is a universal function of  $\lambda/\lambda_c$ , and a plot of  $\nu(\lambda/\lambda_c) = \Psi_\lambda/\Psi_{\lambda_c}$ , which permits determination of  $\Psi_\lambda$  for any wavelength is shown in Fig. 3. For  $\lambda/\lambda_c > 7$  and  $\lambda/\lambda_c < 0.2$  we can use asymptotic formulas for determination of  $\Psi_\lambda$  with 10% accuracy. The form of the dependence of the intensity of radiation on angle also depends on the parameter  $\lambda/\lambda_c$ , and three characteristic dependences for  $\lambda/\lambda_c = 0.1, 1, \text{ and } 10$  are shown in Fig. 4.

8) *Polarization*. The degree of linear and circular polarization defined in the usual way

$$p = (I_{\parallel} - I_{\perp}) / (I_{\parallel} + I_{\perp}), \quad q = 2 \sqrt{I_{\parallel} I_{\perp}} / (I_{\parallel} + I_{\perp}),$$

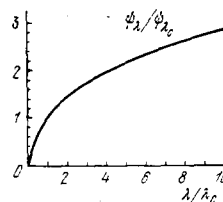


FIG. 3. Universal function  $\nu(\lambda/\lambda_c)$  determining the width of the angular distribution of synchrotron radiation at a given wavelength  $\lambda$  as a function of the parameter  $\lambda/\lambda_c$ .

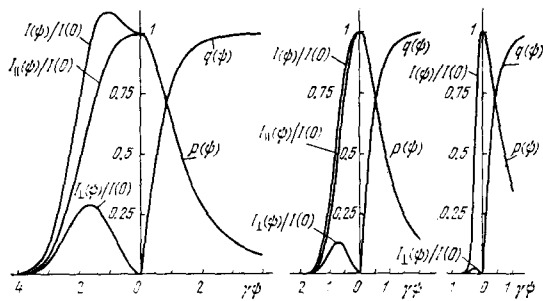


FIG. 4. Dependence of main synchrotron radiation characteristics  $I_{||}$ ,  $I_{\perp}$ ,  $p$ ,  $q$  on vertical angle for parameter values  $\lambda/\lambda_c = 10, 1, \text{ and } 0.1$ .

(where  $I_{||}$  and  $I_{\perp}$  are the intensities of radiation polarized parallel and perpendicular to the orbit plane, and between which there is a phase shift of  $\pm \pi/2$ ) are functions of the wavelength and the vertical angle. In Fig. 4 we have shown the angular dependence of  $I_{||}$ ,  $I_{\perp}$ ,  $p$ , and  $q$  for the three values  $\lambda/\lambda_c = 0.1, 1, \text{ and } 10$ . In the orbit plane ( $\psi = 0$ ) the radiation is completely linearly polarized ( $p = 1, q = 0$ ); in the case when  $\psi > \psi_{\lambda}$  the radiation has elliptical polarization ( $p \rightarrow 0, q \rightarrow 1$ ). The degree of linear polarization, averaged over vertical angle, of radiation at a given wavelength

$$\bar{p}(\lambda) = \frac{\int_0^{\infty} p(\lambda, \psi) N(\lambda, \psi) d\psi}{\int_0^{\infty} N(\lambda, \psi) d\psi}$$

is a universal function of  $\lambda/\lambda_c$ , a plot of which is shown in Fig. 5. In the case  $\lambda \gg \lambda_c$ , we have  $\bar{p} = 50\%$ , and in the other limiting case  $\lambda \ll \lambda_c$ , we have  $\bar{p} = 100\%$ . If we integrate the intensity of radiation over all wavelengths and all vertical angles, then it turns out that the intensity of radiation with polarization parallel to the orbital plane is seven times greater than the intensity of radiation with perpendicular polarization. Therefore the linear polarization averaged over all wavelengths and angles is 75%.

### C. Effect of electron beam parameters on the characteristics of the synchrotron radiation flux

The efficiency of use of SR in various experiments depends not only on the SR intensity, which is determined by the number of radiating particles, their energy, and the magnetic field strength at the point of radiation. A very important effect is exerted by the transverse size of the electron beam at the point of radiation, the angular spread of the electrons in the beam, the length of the bunch, and the minimum permissible distance from the point of radiation to the place where the experiment is carried out. These parameters in many ways determine the quality of the radiation source for the user.

In discussing the effect of the main parameters of the beam of radiating particles on the characteristics of SR, we will assume the source to be an electron storage ring in which the energy, magnetic field, beam

size, and number of particles stored are constant with time. The dimensions  $\sigma_{x,z}$  and angular spread  $\Delta\theta_{x,z}$  of the electron beam in the storage ring depend on the electron beam phase space and the local rigidity of the magnetic focusing structure of the storage ring,

$$\sigma_{x,z} = \sqrt{\epsilon_{x,z} \beta_{x,z}}, \quad \theta_{x,z} = \sqrt{\frac{\epsilon_{x,z}}{\beta_{x,z}}},$$

where  $\beta_{x,z}$  is the effective focal length of the magnetic system at the point of radiation;  $\epsilon_x$  is the radial phase space of the electron beam, determined by the equilibrium quantum excitation and radiation damping;  $\epsilon_z$  is the vertical phase space of the electron beam, determined by the radial phase space and the coupling coefficient of  $x$  and  $z$  oscillations; usually  $\epsilon_z \sim (1/100 - 1/400)\epsilon_x$ .

The characteristics needed by users are obtained by appropriate averaging of the radiation of electrons from a given trajectory over the distribution of electrons in coordinates and angles in the beam. Here the intensity of radiation per unit radial angle integrated over vertical angle remains constant (we recall that so far we are assuming the orbit circular in the entire important part). The spectral distribution of the integrated intensity also varies only slightly. The remaining characteristics change substantially, the more so as the transverse beam size and the angular spread of the electrons are greater.

The angular divergence of the SR beam ( $\psi_{SR\lambda}$ , determined by the angular divergence of the synchrotron radiation  $\psi_{\lambda}$  and the angular spread of the electrons in the beam  $\Delta\theta$ ) increases:

$$\psi_{SR\lambda} = \sqrt{\psi_{\lambda}^2 + (\Delta\theta)^2}.$$

The illumination of a sample placed, as is often the case, rather far from the point of radiation ( $L \gg \sigma_x \psi_{\lambda}$ ) decreases:

$$I_{SR} = I_{\lambda} \frac{\psi_{\lambda}}{\psi_{SR\lambda}} = I_{\lambda} \frac{\psi_{\lambda}}{\sqrt{\psi_{\lambda}^2 + (\Delta\theta)^2}}.$$

The source brightness  $B_{\lambda}$  in a given portion of the spectrum, which is equal to the number of photons radiated per unit time from a unit area of the source into a unit solid angle, is for many applications the main user characteristic of SR. The brightness is essential-

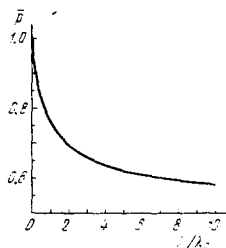


FIG. 5. Dependence of linear polarization, averaged over vertical angle, of radiation at a given wavelength on the parameter  $\lambda/\lambda_c$ .

TABLE I.

Storage ring, city, country	E, GeV	I, A	$\tau$ , h	R, m	$\lambda_c$ , Å	$H_{plan}$ , kOe	$\lambda_{plan}$ , Å	$L_{chap}$ , m	Remarks
1. PETRA, Hamburg, FRG	19	0.09		197	0.16	20	0.93		Planned 1979
2. PEP, Stanford, USA	15	0.1	12	170	0.28				Planned 1980
3. VÉPP-4, Novosibirsk, USSR	7	0.1		33	0.54	20		5	Planned 1977
4. DORIS, Hamburg, FRG	4	0.3		12.1	1			32	
5. SPEAR, Stanford, USA	4	0.09		12.7	1.4				
6. VÉPP-3, Novosibirsk, USSR	2.2	0.12	4-100	6.15	3			2.5	
7. Daresbury, England	2.0	1.0		5.55	4				
8. DCI, Orsay, France	1.8	0.4		3.82	4	45	0.93		Planned 1980
9. ADONE, Frascati, Italy	1.5	0.06	15	5	8.35				
10. VÉPP-2M, Novosibirsk, USSR	0.67	0.1	10-1	1.22	23			2	
11. ACO, Orsay, France	0.56	0.1	40-6	1.11	35			15	
12. INSOR, Tokyo, Japan	0.3	0.1		1.1	228				
13. SURF, Washington, USA	0.24	0.06		0.83	336				
14. TANTALUS-I, Wiscon- sin, USA	0.24	0.06	1-10	0.64	260				
15. N-100, Khar'kov, USSR	0.1	0.25	0.1	0.5	2300			6	

ly determined by the size and angular spread of the electron beam,

$$B_\lambda = \frac{\dot{N}(\lambda)}{\Delta x \Delta z \sqrt{\psi_\lambda^2 + (\Delta\theta)^2}},$$

where  $\Delta_{x,z}$  are the effective radial and vertical size of the source:

$$\Delta_{x,z} \sim \sqrt{4\sigma_{x,z}^2 + R^2(\psi_\lambda^2 + (\Delta\theta_{x,y})^2)}.$$

The degree of polarization of the radiation at a given angle to the direction of radiation falls off for  $\Delta\theta \geq \psi_\lambda$ , and therefore only for wavelengths at which  $\psi_\lambda > \Delta\theta$  is there the possibility of separating radiation with an increased degree of linear or circular polarization by diaphragming the SR beam at a given angle.

*Time modulation* of the synchrotron radiation, which follows the time structure of the electrons grouped in a bunch in the storage ring, is an important factor for some experiments. The length of the electron bunches for a given energy is determined both by the synchrotron radiation itself (the induced radiation damping and the quantization of the energy radiated) and by the storage-ring characteristics—magnetic structure, frequency of the accelerating voltage which compensates the radiation loss of energy, and its amplitude. The minimum length of bunches of existing storage rings is a few centimeters (a further shortening is also possible).

### 3. POSSIBILITIES OF ELECTRON STORAGE RINGS—THE PRINCIPAL SOURCES OF SYNCHROTRON RADIATION

#### A. Comparison of existing electron storage rings with other sources of ultraviolet and x radiation

Originally electron synchrotrons were used as sources of synchrotron radiation,<sup>[21-23]</sup> but at the present time a large part of the experiments with SR are carried out in electron storage rings,<sup>[24-30]</sup> since:

TABLE II.

Source	$\lambda$ , Å	Source size mm <sup>2</sup>	Divergence of radiation	$B_\lambda$ , photons/sec-cm <sup>2</sup> -sr
VÉPP-2M	$(10-10^3)$	$0.5 \times 0.05$	$10^{-3}$	$(10^{23}-10^{24}) \left(\frac{\Delta\lambda}{\lambda}\right)$
Gas discharge Hel lamp	500		$4\pi$	$\sim 10^{20} \left(\frac{\Delta\lambda}{\lambda}\right)$ HeI
VÉPP-3	$(5-0.5)$	$2 \times 0.2$	$2 \cdot 10^{-4}$	$(10^{23}-10^{24}) \frac{\Delta\lambda}{\lambda}$
X-ray tube, $P = 30$ kW	1.54	$0.5 \times 0.5$	$2\pi$	$4 \cdot 10^{20} \left(\frac{\lambda}{\lambda}\right)$ CuK $\alpha$
PETRA	$10^{-1}-10^{-3}$	$8 \times 0.8$	$5 \cdot 10^{-5}$	$(10^{23}-10^{24}) \frac{\Delta\lambda}{\lambda}$
Linear accelerator, 10 MeV, 1 MW	$10^{-3}$	$0.5 \times 0.5$	0.2 sr	$3 \cdot 10^{20} \frac{\Delta\lambda}{\lambda}$

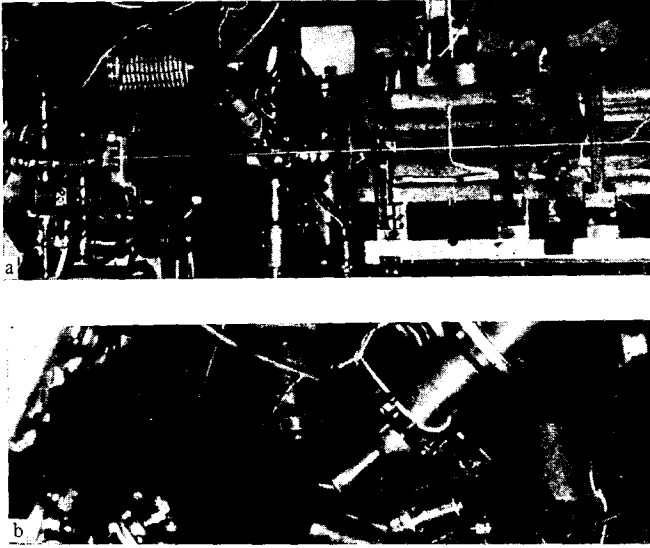


FIG. 6. Photographs of the luminous track of the beam of x-ray synchrotron radiation extracted from the VÉPP-3 storage ring through a beryllium foil into the atmosphere. a) Side view, b) bottom view.

—in storage rings, as a rule, the average current is greater;

—as the result of radiation damping the transverse dimension and angular spread of the beam electrons in storage rings are substantially smaller than in accelerators;

—the stability of the orbit, constancy of energy, and beam intensity in a storage ring greatly simplify the setting up of experiments;

—the large lifetime of a beam in a storage ring (1–100 hours) assures a low level of radiation background around the apparatus, which permits operation at a small distance from the storage ring with a short SR channel.

In Table I we have given the main parameters of existing and planned storage rings used as SR sources.

The obvious qualitative advantages of SR over other sources of vacuum ultraviolet and x radiation (the possibility of separating any wavelength in the range  $10^4$ – $0.1 \text{ \AA}$ , the existence of polarization, good natural collimation, time modulation with a resolution  $\leq 0.1 \text{ nsec}$ , and accurately calculated characteristics) are supplemented in Table II by a quantitative comparison of the brightness of SR from storage rings with sources of other types: a HeI gas-discharge lamp ( $\lambda \sim 500 \text{ \AA}$ ), a sharp-focus x-ray tube with a rotating anode and a power of 30 kW ( $\lambda \sim 1.5 \text{ \AA}$ ), a hypothetical linear accelerator at  $E = 10 \text{ MeV}$  with a power of 1 MW with an optimum heavy liquid metal or rotating converter intercepting the electron beam with the highest possible velocity.

A good picture of a beam of synchrotron radiation can be obtained from the photographs shown in Fig. 6, in which can be seen the luminous track of a beam of x-ray synchrotron radiation emitted from the VÉPP-3

accelerator through a beryllium foil into the atmosphere. A blue luminous band of air ionized by the x-rays is visible at a distance of more than ten meters.

## B. Means for further improvement of storage rings—Specialized sources of synchrotron radiation

Practically all storage rings used at the present time for experiments with synchrotron radiation were developed primarily as installations with colliding electron-positron beams. Therefore, in spite of their high quality, these storage rings are clearly not optimal generators of short-wavelength radiation.

Change of the magnetic structure and introduction of additional devices in already existing accelerators will permit substantial improvement of their characteristics as synchrotron radiation sources.

To analyze the possibilities of increasing the brightness of SR sources, we shall assume that the size of the source is determined only by the dimensions of the electron beam, and the divergence of the SR beam only by the divergence of synchrotron radiation. The size of the electron beam is determined by the electron energy and the characteristics of the magnetic structure of the storage ring<sup>[31]</sup>.

$$\sigma_x^2 = \text{const} \cdot \frac{E^2 \beta_x}{\nu_x^2} \frac{R_{av}}{R},$$

$$\sigma_z = k_{co} \sigma_x \sqrt{\frac{\beta_z}{\beta_x}},$$

where  $k_{co}$  is the  $x$ - $z$  coupling coefficient,  $\nu_x$  is a parameter characterizing the rigidity of the magnetic system ( $\nu_x \sim R_{av}/\beta_x$ ), and  $R_{av} = \Pi/2\pi$  is the mean radius of the storage ring.

When the above assumptions are taken into account the formula determining the brightness of SR (see Sec. C of Part 1) can conveniently be rewritten in the form

$$B_\lambda = \text{const} \cdot \frac{I \eta \lambda^3 k_c \nu_x^2}{k_{co} E \psi_\lambda \sqrt{\beta_x \beta_z}} \frac{R}{R_{av}} \frac{\Delta \lambda}{\lambda}.$$

In generation of SR it is desirable to place in the storage ring orbit special magnets in which the field strength can be changed independently of the main magnetic system. To obtain radiation with the necessary wavelength  $\lambda$  the magnetic field in these magnets must be such that at the existing energy  $\lambda_c \sim \lambda$ . Here  $\psi_\lambda \sim 1/E$ , and

$$B_\lambda = \text{const} \cdot \frac{I \eta \lambda^3}{k_{co} \sqrt{\beta_x \beta_z}} \frac{R}{R_{av}} \frac{\Delta \lambda}{\lambda}.$$

Therefore the source brightness can be increased by using several different means of independently varying the parameters of the magnetic system:

—installation of special correcting systems to decrease the coupling of  $x$  and  $z$  oscillations;

—increasing the rigidity of the focusing system in the radial direction;

—compressing the size of the electron beam ( $\sigma_{x,z} = \sqrt{\epsilon_{x,z} \beta_{x,z}}$ ) in the region of radiation as the result of

reducing the effective focal length of the magnetic system  $\beta_{x,z}$  at the point of radiation, as is done at the interaction points to increase the luminosity of colliding beams (straight sections with low  $\beta$  function); it is useful to decrease the size until the angular spread in the electron beam exceeds the angular divergence of synchrotron radiation.

Another possibility of increasing the brightness of an SR source is use of special regions with large fields of alternating sign (wigglers) installed in the straight sections of the storage ring. The average value of the field in such a wiggler must be chosen as zero. For a short-wavelength wiggler in which the distance between neighboring magnets  $d$  is of the order of the gap between the magnet poles, the magnetic field on the beam axis can be represented with high accuracy in the form

$$H(s) = H_{\max} \cos \frac{\pi s}{d},$$

where  $s$  is the coordinate along the trajectory,  $H_{\max}$  is the field between the poles, and  $d$  is the distance between neighboring magnets. In this case the total SR beam power (integrated over all wavelengths and over vertical and radial angles) from a wiggler of length  $L_{wi}$  will be

$$P_{Lwi} \text{ (W)} = 6.3 \cdot E^2 \text{ (GeV)} H_{\max}^2 \text{ (kOe)} I \text{ (A)} L_{wi} \text{ (m)}.$$

For the condition  $d \gg R/\gamma$  the spectral flux of photons from a wiggler of length  $L_{wi}$  is determined by the universal function  $\eta_{wi}(\lambda/\lambda_m)$  which replaces the function  $\eta(\lambda/\lambda_c)$  used in the case of a circular trajectory:

$$N_{wi}(\lambda) \text{ (photons/sec)}$$

$$= 7.4 \cdot 10^{17} H_{\max} \text{ (kOe)} I \text{ (A)} L_{wi} \text{ (m)} r_{wi} \left( \frac{\lambda}{\lambda_m} \right) \frac{\Delta\lambda}{\lambda},$$

where  $\lambda_m \text{ (\AA)} = 186/E^2 \text{ (keV)} H_{\max} \text{ (kOe)}$ ; a plot of this function is given in Fig. 2.

The angular distribution of the SR beam from a wiggler in the vertical direction is determined in the same way as for the case of a circular trajectory; in the radial direction

$$\psi_{xwi} = 1 \sqrt{1 + (\Delta\theta_x)^2 + \varphi^2(\lambda)},$$

where  $\psi_\lambda$  is the angular divergence of synchrotron radiation,  $\Delta\theta_x$  is the angular spread of the electrons in the beam,  $\varphi(\lambda) = \varphi_{\max} f(\lambda/\lambda_m)$ ,  $\varphi_{\max} \approx 10^{-4} H_{\max} \text{ (kOe)} d \text{ (cm)}/E \text{ (GeV)}$  is the bending angle of the electron beam in the wiggler, and

$$f\left(\frac{\lambda}{\lambda_m}\right) \rightarrow 1 \text{ for } \lambda > \lambda_m,$$

$$f\left(\frac{\lambda}{\lambda_m}\right) \rightarrow 0 \text{ for } \lambda \ll \lambda_m.$$

The maximum radial deflection of the electron beam in a wiggler in real situations is advantageously made small, in order that  $\delta x_{wi} \approx d \varphi_{\max}/2 \ll \sigma_x$ . The effective vertical and radial dimensions of the source are related to its length (the length of the wiggler):

$$\Delta_z = \sqrt{4\sigma_z^2 + L_{wi}^2 (\Delta\theta_z)^2},$$

$$\Delta_x = \sqrt{4\sigma_x^2 + L_{wi}^2 [(\Delta\theta_x)^2 + \varphi^2(\lambda)]}.$$

In optimization of the parameters of a wiggler to maximum brightness in the region of any wavelength  $\lambda$ , the main parameters of the wiggler can reasonably be chosen from the condition  $\lambda \sim \lambda_m$ ,  $\varphi(\lambda) \ll \Delta\theta_x$ ,  $L_{wi} \ll \beta_x$  ( $\beta_x$  is the value of the  $\beta$  function at the point of installation of the wiggler). Such a wiggler in principle permits increase of the brightness of the SR beam by 20–1000 times, approximately. However, it should be noted that installation of a wiggler can substantially affect the parameters of the magnetic system of the storage ring (change of the damping decrement, shift of the betatron oscillation frequencies, appearance of a strong nonlinearity). Therefore it is necessary to consider accurately the question of the effect of a wiggler on the motion of the particles in the storage ring. We note that the effectiveness of use of wigglers in the undulator regime depends greatly on the angular spread of the electrons in the beam. [19]

In designing specialized electron storage rings it is possible to concentrate the main fraction of radiation loss in straight wigglers of this type, choosing the magnetic field in the wigglers and the bending magnets of the storage ring such that the integral of the square of the magnetic field along the wigglers is greater than the integral over the remaining portions of the storage ring. The problem of conversion of high-frequency energy into useful synchrotron radiation is important even for research storage rings, since here tens or hundreds of kilowatts of x-rays are involved. The problem becomes dominant when technological applications are found for synchrotron radiation.

As an example let us consider three storage rings with long straight sections, VÉPP-3, VÉPP-4, and PETRA. In Table III we have given the parameters of the SR beams which can be obtained with use of a wiggler.

In storage rings which are specialized SR sources, in addition to solution of the problems of increasing the source brightness, increasing the SR beam power, and increasing the energy efficiency, it is necessary to consider the possibility of more complete utilization also of other features of SR.

For example, in a storage ring it is useful to provide straight sections where the vertical size is enlarged but the angular spread in the electron beam is reduced to a value substantially less than the divergence of synchrotron radiation (straight sections with high  $\beta$ ). Extraction of a beam of synchrotron radiation from this

TABLE III.

	$H$ , kOe	$L$ , m	$\lambda$ , Å	$h\nu$ , keV	$I$ , A	$\bar{P}$ , kW
VÉPP-3, $E=2.2$ GeV	50	1	0.8	15	0.1	5
VÉPP-4, $E=7$ GeV	50	5	0.076	160	0.1	400
PETRA, $E=19$ GeV	50	5	0.01	$1.2 \cdot 10^3$	0.1	2500



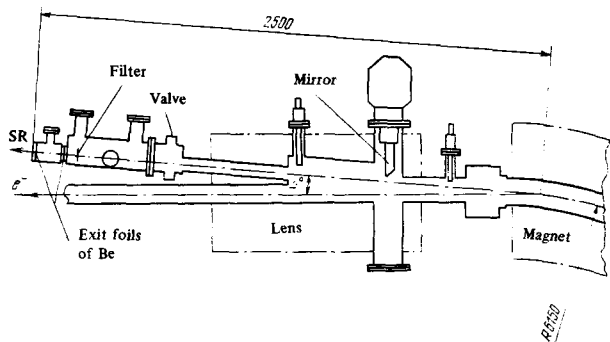


FIG. 7. Scheme for extraction of x-ray synchrotron radiation from the VEPP-3 storage ring (dimensions in millimeters).

region, using geometrical diaphragming of the SR beam, will permit separation of radiation with a high degree of linear and circular polarization not only in the region of vacuum ultraviolet, but also in the hard x-ray region.

To obtain time modulation of the intensity of SR over a wide range of times ( $10^{-11}$  – 1 sec) in a specialized storage ring SR source, it is necessary to provide:

- a high-frequency system which permits bursts of length 0.1–1 cm to be obtained;

- a special system of synchronization to provide operation of the storage ring in the single-bunch mode, or in a mode with  $n$  bunches repeated with a time interval  $\Delta T = T_{\text{rev}}/n$  ( $T_{\text{rev}}$  is the period of revolution of particles in the storage ring);

- in the vicinity of the point of radiation one must have the possibility of introducing a local pulsed distortion of the orbit, which, by diaphragming the SR beam, permits any arbitrary time modulation of the SR intensity to be obtained.

In development of electron storage rings which are specialized sources of synchrotron radiation, the simplicity, reliability, and relatively low cost become very important aspects. Such storage rings can undoubtedly be much simpler than existing storage rings developed for experiments with colliding electron-positron beams. It is true that sources in the x-ray region (wavelengths of the order of an Å and shorter) will remain very large installations which it is reasonable to construct for large scientific centers. A source with an upper limit of the radiated spectrum of tens of angstroms can be made quite accessible for individual institutes and large laboratories.

### C. Features of performance of experiments with synchrotron radiation in storage rings

In spite of the difference in storage rings, determined mainly by the energy, the size of the storage ring, and the location of the areas used for experiments with SR, and in spite of the great diversity of the experiments themselves, it is possible to make several general remarks which are important for experimenters planning use of synchrotron radiation.

1) *Connection of the experimental equipment with the vacuum system of the storage ring.* Electron storage rings require for successful operation a high vacuum in the chamber ( $1 \times 10^{-9}$  Torr or better) and complete avoidance of entry into the chamber of organic compounds (oils and greases, which are still used in low-vacuum technique, etc.). Therefore it is practically obligatory to have excellent separation in vacuum of the experimental regions and the storage-ring chamber.

For radiation with wavelength shorter than 5 Å it is reasonable to have complete separation with use of a beryllium foil of thickness 0.1–0.3 mm. In Fig. 7 we have shown a diagram of the channel for extraction of SR with  $\lambda > 5$  Å from the VEPP-3 accelerator.<sup>[25]</sup> The channel contains stub-type radiation probes which can completely cut it off, a high-vacuum valve, after which is attached the exit chamber of the channel, a magnetic ion pump, and an exit window of beryllium 0.15 mm thick. The exit compartment of the channel is terminated by a fore-vacuum region and second exit foil of beryllium of the same thickness. The purpose of this region is to assure additional protection of the vacuum chamber of the storage ring from the atmosphere in the case of mechanical, radiation, or chemical damage of one of the exit foils. In addition, at high intensities an additional beryllium absorber of variable thickness is placed in front of the exit foil, so as to absorb the long-wavelength portion of the radiation and to reduce the thermal load on the outer foil.

For radiation with wavelength  $\lambda > 5$  Å, direct connection of the storage-ring vacuum chamber (working vacuum  $\leq 10^{-9}$  Torr) with the vacuum chamber of various kinds of experimental apparatus (working vacuum  $\sim 10^{-6}$  Torr) is necessary. In this case it is most efficient to use differential pumping, accomplishment of which is facilitated by the small size of SR beams with wavelength shorter than 1000 Å. In Fig. 8 we have shown a diagram of the vacuum channel for extraction of SR from the storage ring VEPP-2M.<sup>[26]</sup> Three sections of differential pumping are installed in the channel, each of which includes a portion of the channel with low conduction, a buffer volume, a nitrogen trap with a nitrogen storage time of several days, and a magnetic ion pump. In addition, the channel contains two high-vacuum gate valves and two emergency valves with an operation time of 0.1 sec.

2) *Radiation conditions.* As the result of the large lifetime of the beam in a storage ring (1–100 hours)

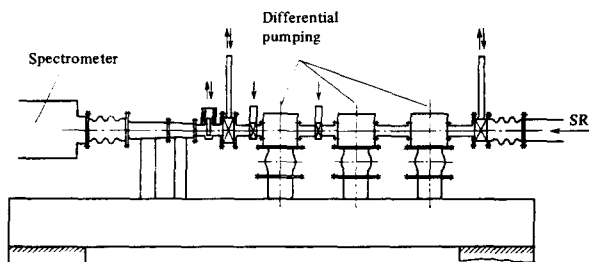


FIG. 8. Arrangement of vacuum channel for extraction of ultraviolet and soft x-ray radiation from the VEPP-2M storage ring.

the loss of particles per unit time is many orders of magnitude ( $10^7$ – $10^5$  times) less than in ordinary accelerators. Therefore there is practically no induced activity present around the storage ring, and the radiation background due to high energy electrons,  $\gamma$  rays, and neutrons is extremely low. This permits apparatus for experiments with synchrotron radiation to be placed in the immediate vicinity of the storage ring, using short SR channels of length 1–10 m.

To provide safety for experimenters, whose presence at the apparatus is desirable at the time of tuneup and adjustments, it is necessary to localize the place of particle loss in various emergency situations (turnoff of the high frequency system, failure in the magnetic system, etc.) by installation of special probes which limit the aperture at a location far from the SR channel. It is also possible to use a rapidly introduced probe (time 1–10 msec) operating in emergency situations, or deflectors which dump the beam in the time of the order of a revolution.

In addition, it is necessary to install in front of apparatus used in experiments with SR a shield which in the event of a beam dump would get rid of the secondary radiation and avoid the possibility of obtaining a large local dose in the very unlikely case of direct incidence of the beam into the region of the experimental apparatus.

Much greater danger is presented by the SR beam itself. For example, at the exit of the SR channel of the VEPP-3 storage ring the local dose can reach  $\sim 10^5$  roentgens/sec. The levels of scattered radiation near the open beam are  $10^2$ – $10^3$  roentgens/hour (at a distance of 0.5 m). However, as a result of the low energy of the synchrotron radiation photons ( $h\nu < 40$  keV), a radiation shield of lead of thickness 2–5 mm turns out to be sufficient in practice.

3) *Use of experimental apparatus appropriate for the radiation source.* In effective utilization of the new sources of synchrotron radiation, it is of great value to choose experimental arrangements which take into account the specific properties of SR, and also to use optimal systems for monochromatization and focusing of the SR beam, and to use contemporary methods of photon detection and analysis of the data obtained.

Some examples which illustrate the effectiveness of optimal choice of the experimental arrangement will be given later under the discussion of various experiments utilizing SR. Here we note only that optimal choice of apparatus design taking into account the properties of SR can not only increase the flux of useful photons for a given experiment, but also can greatly improve the effect/background ratio (see the example of decrease of Compton background as the result of use of polarization of the radiation in x-ray fluorescence analysis, and the example of use of time modulation of radiation in Mössbauer experiments).

Another very important choice is that of the monochromators, which are necessary to separate the wavelength used from the continuous spectrum of SR. On

the one hand, it is always desirable to have a monochromator which transmits the maximum value of  $\Delta\lambda$  permissible for a given experiment, since the total number of useful photons is proportional to  $\Delta\lambda$ . On the other hand, the difficult problem arises of spoiling the phase density of the photon beam by the crystal monochromators, for which  $\Delta\lambda/\lambda$  is equal to the angular spread  $\Delta\lambda/\lambda \sim \Delta\theta_M$  introduced into the photon beam. Therefore in experiments where good angular resolution is required (x-ray holography, small-angle diffraction, various types of x-ray microscopy, and so forth) it is necessary to use the two most effective monochromator locations, either as close as possible to the source, or in front of the detector.

With the crystal monochromator located near the source,  $\Delta\theta_M$  should be less than the radiation angles  $\psi_\lambda$  i. e.,  $\Delta\lambda/\lambda < \psi_\lambda$ . For the x-ray region this corresponds to  $\Delta\lambda/\lambda < 10^{-3}$ . If for technical reasons the monochromator cannot be placed close to the source, or if it is desirable to use the widest possible region of the spectrum, the monochromator must be placed near the detector.

In this case a value  $\Delta\theta_M = \delta\theta L_0/L_M$  is permissible, where  $\delta\theta$  is the required angular resolution,  $L_0$  is the distance from the sample to the detector, and  $L_M$  is the distance from the monochromator to the detector. The minimum value of  $L_M$  is determined by the necessity of spatial separation of the various reflections coming simultaneously from the crystal. The crystal monochromator must withstand the large heat load resulting from the SR beam absorbed in the crystal (up to 100 W/cm<sup>2</sup> in existing accelerators) and must have the necessary time stability and resistance to radiation.

It is also necessary to recall that the radiation spectrum extends practically without limit into the short-wavelength region, falling off only exponentially for wavelengths shorter than  $\lambda_{max}$ . Therefore it is necessary in monochromatization of synchrotron radiation to be concerned constantly with suppression of short-wavelength harmonics (spectra of higher orders). This problem is solved by several means:

- working at the edge of the SR spectrum;
- selection of a crystal or specially constructed diffraction grating in which quenching of certain orders of reflection occurs;
- use of two successive reflections from crystals, for which the correction to the Bragg angle as the result of the refractive index is different for the main line and for the harmonics;
- use of detectors with energy resolution sufficient for discrimination against photons with twice the energy;
- use of a total-external-reflection mirror, which does not reflect radiation with  $\lambda < \lambda_i$  for  $\theta > \theta_i$  ( $\theta_i = f(\lambda)$  is the critical angle for total external reflection).

A total-external-reflection mirror can be used successfully also for focusing the beam, provided that the mirror roughness is  $\delta h < \lambda/\theta_i$ . To provide focusing the mirror must have a radius of curvature

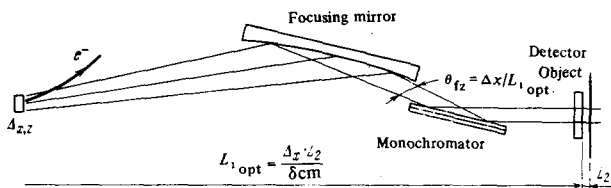


FIG. 9. Diagram showing use of synchrotron radiation for contact microscopy.

$$R = \frac{2 L_m L_d}{(L_m + L_d) \theta_i},$$

where  $L_m$  is the distance from the point of radiation to the mirror and  $L_d$  is the distance from the mirror to the detector.

The length of the mirror must be such as to reflect the photon flux traveling in the necessary angular interval  $\Delta\psi$ :

$$l \geq L_m \frac{\Delta\psi}{\theta_i}.$$

Focusing of an SR beam is also achieved successfully by focusing monochromators (a plane monochromator with an oblique cut, or curved crystals).

The use of synchrotron radiation as a fundamentally new high-power source of ultraviolet and x radiation requires adequate apparatus for performance of experiments: semiconductor detectors with high energy resolution, coordinate wire proportional chambers, precision monochromators, and photoelectron spectrometers. The rapid flow of information requires that it be continually fed to a computer and analyzed during the course of the experiment, as is widely done in high energy physics. Use of such apparatus and techniques is also useful in work with ordinary radiation sources. The collaboration in experiments utilizing SR with laboratories concentrated around electron-positron storage rings makes this step much more natural, trouble free, and rapid. [18, 32, 33]

#### 4. USE OF SYNCHROTRON RADIATION FOR X-RAY MICROSCOPY

The appearance of x-ray sources many orders of magnitude more intense than existed previously requires a new look at the possibilities of various forms of microscopy in this wavelength region ( $\lambda \leq 100 \text{ \AA}$ ).

##### A. Contact microscopy

The logically simplest variant of microscopy is contact microscopy (Fig. 9). An almost parallel beam of white or monochromatized SR passes through an object located at a distance  $L_1$  from the point of radiation and hits a detector located a small distance  $L_2$  from the object.

Contact microscopy is based on the use of the high resolution of the detectors (the resolution of modern detecting devices reaches several thousand lines per millimeter, and the resolvable dimensions approach

1000  $\text{\AA}$ ). One can use as a detector the photographic emulsions developed for nuclear experiments and optical holography, and new special holographic materials which change their refractive index on irradiation. Scanning can be accomplished either by means of an optical microscope or by use of laser techniques.

The need of using such high-resolution detectors in contact microscopy makes it impossible today to feed the information directly (on line) to a computer, although the creation of detecting media not requiring development and the use of laser readout may change this situation.

In contact microscopy the contrast of the image is determined by the modulation of the absorption in the sample being studied. With use of analog detectors (detectors without photon counting) the minimum detectable modulation is likely to be several percent. Use of this type of detector greatly reduces the sensitivity of the method, since two to three orders of magnitude more photons (for example, per area of resolved element) are required for formation of an image than the number determined by the statistical noise of a receiver recording each photon incident on it.

The spatial resolution in contact microscopy  $\delta_{cm}$  is determined by the detector resolution, the geometrical characteristics of the radiation source, the monochromator characteristics (if it is used), and by the diffraction of the radiation with wavelength  $\lambda$  by the object details being studied of size  $\delta_{cm}$ :

$$\delta_{cm}^2 = \delta_r^2 + \left( \frac{\Delta_{x,z}}{L} L_2 \right)^2 + \delta\theta_M^2 L_2^2 + L_2 \lambda,$$

where  $\delta_r$  is the detector resolution,  $\Delta_{x,z}$  is the size of the radiation source, and  $\delta\theta_M$  is the angular width of the reflection curve of the crystal monochromator, which is determined by the mosaic in structure of the crystal and is usually related to the spectral width of the radiation separated by the monochromator,

$$\delta\theta_M \sim \frac{\delta\lambda}{\lambda}.$$

Therefore to obtain x-ray microphotographs with spatial resolution  $\delta_{cm}$  it is necessary to have a detector with  $\delta_r < \delta_{cm}$ , to use a monochromator with  $\delta\theta_M \leq \delta_{cm}/L_2$ , and to choose the distance from the radiation source to the subject  $L \geq (\Delta_x/\delta_{cm})L_2$ . To obtain the best possible illumination of this subject it is necessary to choose  $L_{opt} = (\Delta_x/\delta_{cm})L_2$ , and since usually in a storage ring  $\Delta_x \gg \Delta_z$ , to obtain the maximum number of photons per resolved element of this subject it is necessary to use focusing of the radiation in the vertical direction. Here there will arrive at the area of the resolved element  $\delta_{cm}^2$  a number of photons per second  $\dot{N}_\delta$  equal to

$$\dot{N}_\delta = \frac{d\dot{N}}{d\Omega} \frac{\delta_{cm}^2}{L_{opt}^2} = \frac{d\dot{N}}{d\Omega} \frac{1}{\Delta_x \Delta_z} \frac{\delta_{cm}^2}{L_2^2} = B_\lambda \frac{\delta_{cm}^2 \Delta\lambda}{L_2^2 \lambda}.$$

In order that diffraction in the details of the subject with size  $\delta_{cm}$  not spoil the resolution,  $L_2$  must be no greater than  $\delta_{cm}^2/\lambda$ . It is interesting to note that with this maxi-

TABLE IV.

$\delta_L, \mu$	$\lambda, \text{Å}$	$L_2, \text{mm}$	$\Delta\theta = \frac{\Delta\lambda}{\lambda}$	$N_0^{\text{max}}, \text{photon/sec} \cdot \delta^2$
0.3	1	1	$3 \cdot 10^{-4}$	$1.5 \cdot 10^4$
2	10	40	$2 \cdot 10^{-3}$	$1.6 \cdot 10^6$
2	10	4	$2 \cdot 10^{-3}$	$3 \cdot 10^6$

imum permissible detector distance the number of useful photons per area of resolved element is determined only by the radiation source,

$$\dot{N}_0 = B_\lambda \lambda^2 \frac{\Delta\lambda}{\lambda}$$

Here the size of the illuminated portion of the sample along the vertical is  $\Delta z_{\text{sam}} = (\delta \Delta z / \lambda) \psi_\lambda$ , and the number of resolvable elements along the vertical direction is  $\eta_z = (\Delta z / \lambda) \psi_\lambda$ . The selection of an optimal monochromator having  $\Delta\theta_M = \Delta\lambda / \lambda = \delta / L_2$  permits the maximum illumination to be obtained.

For  $\Delta\lambda / \lambda \leq 10^{-2}$  it is possible to use crystal monochromators, but to work with a wider range of wavelengths it is obviously necessary to resort to a combination of absorbers and total external reflection. The development of high resolution detectors with selective sensitivity to a certain wavelength region is possible. Use of detectors with good energy resolution in contact microscopy is not possible today.

As an example we shall consider the possibilities of contact microscopy in the SR beam of the accelerator VÉPP-3, which at  $E = 2.2$  GeV and a current of 100 mA has a brightness  $B_\lambda = (0.2-1) \times 10^{24} \Delta\lambda / \lambda$  (photons/sec-cm<sup>2</sup>) in the range  $\lambda = 0.5-10$  Å (Table IV).

The large values of  $N_0^{\text{max}}$  should permit an x-ray microphotograph of an object to be obtained in a time  $10^{-5}-10^{-1}$  sec. The high brightness of synchrotron radiation sources permits x-ray microphotographs to be obtained in short times with high spatial resolution for a comparatively small value  $L_2 \sim 1-10$  mm, which provides the following possibilities:

- to carry out mapping of various objects, including biological objects, in a special container which has sufficient uniformity of absorption at the working wavelength;
- using special kinematic gates to take microscopic motion pictures;
- to carry out greatly foreshortened mapping of an object with subsequent stereoscopic interpretation.

The possibility of separating any wavelength from the spectrum of synchrotron radiation permits working in the vicinity of the  $K$  absorption edges ( $\lambda = 0.5-20$  Å) of intermediate and heavy elements present in the sample. The difference pattern obtained from mapping a sample exactly at the  $K$  edge and just below it in energy permits the image contrast to be greatly increased.

The most convenient region of wavelength for contact microscopy is  $0.5-4$  Å, for which there are detectors

with high resolution and vacuum operation is not required. The transition to longer wavelengths, possibly, will be justified for the purpose of obtaining good contrast in mapping of extremely thin samples (such as single-cell layers). To improve the contrast it is possible, as in optical microscopy, to use tinting of the necessary details by highly absorbing materials.

An illustration of the possibility of x-ray contact microscopy is the work<sup>[34]</sup> carried out jointly by the staffs of the Institute of Automation and Electrometry and the Institute of Nuclear Physics, Siberian Division, USSR Academy of Sciences, in which test objects (a nickel grid with a step of  $30 \mu$  and a width and thickness of wires  $7 \mu$ ) were projected onto chalcogenide glass films by nonmonochromatized x-ray synchrotron radiation from the storage ring VÉPP-3 ( $\lambda = 0.5-4$  Å). Under the action of x-rays a change of refractive index for visible light occurs in these films; no development is required. The resolution of the films is better than 5000 lines/mm. Control of the quality of the image recorded and selection of exposure is accomplished during the exposure on the basis of the diffraction pattern arising from a laser beam in the phase lattice which appears.

In Fig. 10 we have shown an enlarged image of the phase lattice observed in the microscope by the phase-contrast method. The blurring of the lattice image does not exceed  $0.5 \mu$ , the exposure time was several seconds (storage-ring current 50 mA,  $E = 2$  GeV, distance from point of radiation to sample  $\sim 10$  m, distance from sample to detector  $\sim 1$  mm).

## B. X-ray topography

Related to contact microscopy is the x-ray topography of single crystals, which permits direct observation of images of various defects and obtaining of information on the real structure of crystals. Study of the internal structure of reflections obtained at the Bragg angles permits study of defects occurring only near the surface of the crystals. In transmission work (as in Laue photographs) it is possible to study the structure of thin crystals over their entire cross section.

With use of x-ray tubes as the source of radiation, the time required to obtain topograms is several days (with a power  $P = 1$  kW, MoK $\alpha$  radiation, topogram size  $8 \times 8$  mm).<sup>[35]</sup> It should also be noted that the interpre-

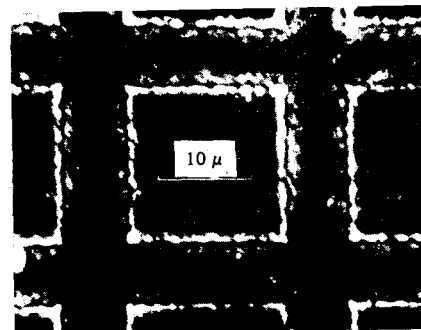


FIG. 10. Image of test object on chalcogenide glass film, obtained by contact projection.



FIG. 11. X-ray topogram of quartz crystal. The spatial resolution is better than 1 micron; edge dislocations are visible.

tation of topograms up to the present is based on qualitative treatments, and some details of the topograms remain unexplained.<sup>[36]</sup> To a considerable extent this is due to the fact that incoherent illumination is used in the experiments and the information obtained is very hard to interpret. Practical realization of coherent illumination with use of x-ray tubes is impossible, since this would lead to a substantial increase in the already very long times for obtaining topograms.

Therefore the switch to synchrotron radiation is extraordinarily effective for x-ray topography, since:

- the time required is greatly reduced ( $\sim 10^3 - 10^5$  times) with a simultaneous improvement in the spatial resolution (estimates of the achievable resolution and exposure time are close to those given for contact microscopy);
- the high brightness of SR permits topograms to be obtained with coherent illumination (see Section E of Chapter 4);
- use of the continuous spectrum of SR permits simultaneous recording of several reflections (up to 10–20) without requiring precise adjustment of the crystal;
- the natural polarization of synchrotron radiation opens up new experimental possibilities.

In Fig. 11 we have shown a photograph of a topogram of quartz obtained by workers at the Institute of Crystallography, USSR Academy of Sciences, with use of SR from the VÉPP-3 storage ring. The topogram was obtained by the Laue method in a white beam of SR. The distance from the point of radiation to the sample was  $\sim 12$  m, and the distance from the sample to the film 12 cm. The sample was a plate of thickness 0.8 mm. The time required to obtain the topogram was  $\sim 5$  sec (for a storage ring current of 20 mA and an energy 2 GeV) and the spatial resolution is better than  $1 \mu$ . Edge dislocations can be seen in the topogram.

### C. Projection microscopy

Use of this form of microscopy permits avoidance of use of a detector with high resolution equal to the required resolution in the object. The sample studied is illuminated by x-ray photons originating from a diaphragm of size  $\delta_d$  located at a distance  $L_2$  from the object. The magnified image of the object is projected on a detector having resolution  $\delta_{det}$  placed at a distance  $L_{det}$  beyond the sample.

The spatial resolution in projection microscopy is

determined by the size of the diaphragm and is limited by diffraction in the sample details studied of size  $\delta_{pm}$ :

$$\delta_{pm}^2 = \delta_d^2 + \lambda L_2 + \frac{\delta_{det}^2 L_2^2}{L_p^2}.$$

To obtain the limiting resolution equal to the diaphragm size, the detector must be located quite far away:

$$L_{det} \geq \frac{\delta_{det}}{\delta_{pm}} L_2.$$

The distance  $L_2$  must be chosen such that diffraction in an element of the sample with size  $\delta_{pm}$  gives angles less than the angles subtended by the diaphragm at the sample:

$$L_2 \leq \frac{\delta_{pm}^2}{\lambda}.$$

Let us now estimate the maximum number of useful photons (i. e., photons which can be collected in an aperture of size  $\delta_{pm}$ ) and the number of photons which can hit a resolved element of size  $\delta_{pm}$  on the sample.

If we do not utilize focusing onto the diaphragm and if we place the diaphragm in the immediate vicinity of the source, a number of photons of the order  $B_\lambda \delta_{pm}^2 \psi_{SR} \lambda^{\Delta\lambda/\lambda}$  will pass through a diaphragm of area  $\delta_{pm}^2$  in one second. Reasonable use of focusing elements, which can provide focusing with angles  $\theta_f \gg \psi_{SR}$ , will give a number of useful photons  $B_\lambda \delta^2 \theta_f^2 (\Delta\lambda/\lambda)$  (here one of the focusing elements can also be at the same time the monochromator).

The maximum illumination (on  $\delta_{pm}^2$ ) of the sample will be achieved in the trivial case when a thin sample is placed right next to the diaphragm; this case is interesting only in scanning microscopy and will be discussed below. In a truly projection mode the minimum distance from the diaphragm to the subject is determined by the desired field of view, which can be characterized by the number of resolved elements in each of the directions,  $n_{x,z}$  (accordingly the size of the illuminated portion of the sample in one direction is  $\Delta_{sam} = n\delta$ ). Then onto one resolved element there will fall in one second  $\dot{N}_\delta = B_\lambda (\theta_f/n)^2 \Delta\lambda/\lambda$  photons for a distance from the diaphragm to the subject

$$L_2 = \frac{n\delta_{pm}}{\theta_f}.$$

However, this distance must not be greater than permitted by the diffraction spreading in the details of the object,  $\sim \delta_{pm}^2/\lambda$ . For this maximum permitted distance the number of photons per second arriving at a resolved element is

$$\dot{N}_\delta = B_\lambda \lambda^2 \frac{\Delta\lambda}{\lambda},$$

and the number of resolved elements in each direction will be

$$n = \frac{\theta_f \delta_{pm}}{\lambda}.$$

This is the maximum possible number if no use is made of special scatterers inside the diaphragm. The number of resolved elements could be increased by placing inside the diaphragm some type of weakly absorbing scatterers (here the sample illumination decreases quadratically with increase of the number of resolved elements).

In analysis of the possibilities of projection microscopy with SR in the x-ray region it is necessary to have in mind that, as the result of the weak absorbing ability of materials at these wavelengths, the diaphragm will consist of a long channel in an absorbing material and for resolutions on the micron scale  $\theta_f$  cannot be much greater than  $10^{-2}$  (although here it is also possible to use funnel-shaped channels with large angles, provided that the total number of photons passing through the material is substantially less than the number passing through the opening).

The possibility of using detectors with poor resolution in projection microscopy permits a switch to modern coordinate-sensitive detectors (of the type of wire proportional chambers) with a photon-counting efficiency close to unity. This permits the distinguishable image contrast to approach the level determined by statistical fluctuations. An important advantage is also the easy possibility of connecting these detectors on line with a computer.

The energy resolution of contemporary coordinate-sensitive detectors is very poor, and therefore to select a narrow range of utilized wavelengths it is necessary to use monochromators. From this point of view it will be very important (and it currently appears possible) to create, by means of semiconductor integrated microelectronics, detectors having both sufficient coordinate resolution (number of resolved elements in one direction  $\sim 100$ ) and energy resolution (let us say, of the order of a percent). We recall that single semiconductor detectors with energy resolution  $\sim 1\%$  have already been developed in the x-ray region.

The ease of working on line with a computer in projection microscopy greatly simplifies the obtaining of information on the absorption of the sample at various wavelengths, which permits information to be obtained on the distribution of heavy and intermediate elements in the sample, by means of the  $K$  absorption edges (with the same spatial resolution  $\delta$ ).

The brightness (in the direction of radiation) of contemporary SR sources greatly exceeds the brightness of the best microfocussing x-ray tubes even for their characteristic radiation. However, the isotropic nature of the radiation from x-ray tubes leads to the result that for projection microscopy the total number of useful photons (in the characteristic lines) approaches that given by an electron storage ring (it is true that the minimum size of the radiator in a tube will be no less than the diffusion length for stopping the fast electrons in the x-ray tube). Therefore the main advantage of synchrotron radiation in this form of microscopy remains the possibility of working at any wavelength, and only in the future is there the hope of going over to detectors with

high energy resolution which will greatly increase the number of actually utilized photons.

#### D. Scanning microscopy

One useful form of x-ray microscopy which has already been accomplished in SR beams<sup>[37]</sup> is scanning microscopy. In this scheme a flux of photons limited by a diaphragm with size  $\delta$  hits a closely placed sample and the result of interaction of the photons with the sample material is detected. The moment of detection is synchronized with the location of the diaphragm, which scans the sample.

Scanning can be accomplished either by moving the sample with a fixed diaphragm, photon-collection system (source and focusing elements), and detecting apparatus, or with a fixed object by movement of the diaphragm and, for a large scanning field, of the entire remaining apparatus (the detecting part can often remain fixed). For high scanning rates the latter system is obviously preferable. For very low scanning rates it is possible to use just micromechanisms. For high rates it is reasonable to use various electromagnetic-mechanical phenomena such as the piezoelectric effect. Specific arrangements can be quite diverse.

The spatial resolution in scanning microscopy is determined by the diaphragm size  $\delta$ , for the condition that the angles of incidence of the radiation on the diaphragm  $\theta_f$  and the diffraction angles  $\lambda/\delta$  give a magnification of the dimensions less than  $\delta$  at a distance  $L_2$  from the diaphragm to the exit surface of the sample:

$$\delta_{sm}^2 = \delta^2 + \theta_f^2 L_2^2 + \frac{\lambda^2 L_2^2}{\delta^2}.$$

The total number of useful photons passing through the diaphragm per second for optimal focusing of the SR beam ( $\theta_f = \delta/L_2$ ) will be no greater than  $N_{\Sigma} = B_{\lambda}(\delta^4/L_2^2)\Delta_{\lambda}/\lambda$ .

With use of the limiting sample thicknesses permitted by diffraction, the total number of photons per second will be no greater than

$$N_{\Sigma}^{dif} = B_{\lambda} \lambda^2 \frac{\Delta_{\lambda}}{\lambda}.$$

If the interesting region of the sample has an area  $\Delta^2$ , then the number of photons per second reaching a resolved element of area  $\delta^2$ , averaged over the scanning period, will be no greater than

$$\dot{N}_{\delta} = \frac{N_{\Sigma}}{n^2},$$

where  $n = \Delta/\delta$  is the number of resolved elements of the sample in one direction.

An important advantage of scanning x-ray microscopy (as in the case of scanning electron microscopy) is the possibility of detection of all  $\gamma$  rays from interaction of the radiation with the sample, which gives the possibility of obtaining very rich information on the sample. Particularly extensive possibilities exist for simultaneous modulation of the incident photon energy, which is

possible as the result of the continuous spectrum of SR. In principle it is possible to extend the experiment also to rotation of the sample around axes perpendicular to the incident beam to obtain a three-dimensional pattern.

By studying the dependence of the incident-beam absorption coefficient on the diaphragm coordinate and photon energy, it is possible to obtain the distribution of chemical elements over the sample, by observing the  $K$  and  $L$  absorption edges. The required picture can be obtained by using a continuous spectrum of radiation incident on the diaphragm and using detectors with energy resolution  $\sim 1\%$ . By using radiation which has been well monochromatized beforehand, it is possible to obtain a representation of the distribution of the chemical state of these elements, by studying the fine structure of the absorption edges (see Chap. 6). In studying the absorption in samples with very low concentrations of the interesting elements it is important to tune out the secondary photons (mainly from luminescence), which can be accomplished by detecting only photons traveling in the incident-beam direction and setting the energy-discrimination threshold between the energies of the luminescence and incident photons.

Information on the distribution of elements over the sample can be obtained also by detection of the luminescence photons (the characteristic radiation of the interesting elements). The characteristic features of synchrotron radiation permit the sensitivity of this method to be greatly increased and correspondingly the level of measurable concentrations of elements to be decreased (see Chap. 8 for a discussion of the means of decreasing the background determined by coherent and Compton scattering of the primary photons).

Very valuable information on the local structure of the sample can be obtained by using a scanning diaphragm in combination with various apparatus for x-ray structure analysis, working on line with a computer.

Some useful information can be obtained by measuring the number and energy of the secondary electrons as a function of the diaphragm location. Here two groups of quasimonoenergetic electrons will be informative: photoelectrons and Auger electrons. The depth of the electron yield is small ( $\sim 1 \mu$  for 10 keV), and therefore we can obtain from them information on internal regions of the samples, mainly for rather heavy elements. By using low-energy electrons it is possible to obtain a microdistribution of elements over the sample surface.

Comparing the possibilities of scanning x-ray microscopy (we have in mind the penetrating wavelength range) and the related scanning electron microscopy, we note only the following. X-ray microscopy, in contrast to electron microscopy, permits complete separation of the sample and the radiator in the vacuum space, and, in detection of x-ray photons, also location of the sample under convenient nonvacuum conditions. In detection in the two kinds of microscopy of the characteristic radiation of interesting elements per identical number of secondary luminescence photons, 3-4 orders of magnitude less radiation exposure of the sample is required in the x-ray case than in the electron

case. This useful fact can be decisive in many cases.

As an example we can give the main characteristics of the scanning x-ray microscope used in the beam of the CEA storage ring.<sup>[37]</sup> The diaphragm dimension was  $2 \mu$ , the scanning motion was carried out at a rate of one step per second, the counting rate with a  $2\text{-}\mu$  aperture was  $\sim 10^4 \text{ sec}^{-1}$  from a sample of optimal thickness, forming of the complete pattern occupied a time of 1-10 min, and the radiation dose received during the exposure was  $\sim 100$  rads. The sensitivity was  $\sim 10^{-6} \text{ g/cm}^2$ . It should be noted that these characteristics are not the best possible ones and apparently will be substantially improved in the future in other storage rings.

### E. Holographic microscopy

With the advent of such bright x-ray sources, qualitatively new prospects are opened up for x-ray microholography.<sup>[30, 39]</sup> When speaking of x-ray holography, we will have in mind here small-angle holography (hologram angle  $\theta_h \ll 1$ ) and correspondingly a resolution at the sample  $\delta \approx \lambda/\theta_h \gg \lambda$ .

The most natural scheme in x-ray holography appears to be one similar to the Young experiment.

This scheme of lensless Fourier holography was proposed by Stroke in 1965.<sup>[45]</sup> If it is known that one of the diaphragms is an aperture with diameter  $\delta$  (which can be determined from the width of the diffraction peak by a separate exposure of this diaphragm), and the sample being studied is placed at the second diaphragm, then from the interference pattern observed in the detector plane it is possible to reproduce the wave leaving the object (i. e., to learn the distribution of both amplitudes and phases). Consequently it is necessary to assure that the interference pattern beyond the plane of the sample and illuminator (condenser) not be spoiled. This requires that the spread in the angles of incidence on the object and the illuminator of the almost plane waves not be too large. If the maximum distance between the interfering points in this plane is  $\Delta_0$ , then the angle between neighboring interference peaks is at least  $\lambda/\Delta_0$ . Therefore, if the spread in the angles of arrival  $\theta_{\epsilon, \tau}$  is less than this value, the interference pattern will not be smeared for this reason, i. e., it is required that

$$\frac{\lambda}{\Delta_0} > \theta_{\epsilon, \tau} = \frac{\lambda_{x, \epsilon}}{L_1}.$$

The quantity  $\Delta_{\epsilon, \tau} = \lambda L_1/\Delta_{x, \epsilon}$  is consequently the corresponding transverse dimension of the region of coherent radiation.

For formation of an interference pattern it is necessary to select sufficiently monochromatic photons. The required monochromaticity  $\Delta\lambda/\lambda$  is determined, on the one hand, by the distinguishability of the fine-scale maxima (angle between maxima  $\lambda/\Delta_0$ ) at the edge of the hologram (angle  $\lambda/\delta$ ), which corresponds to a difference in path in comparison with the center  $(\Delta_0/\delta)\lambda$  and which accordingly requires a monochromaticity

$$\frac{\Delta\lambda}{\lambda} \ll \frac{\delta}{\Delta_0}$$

On the other hand, for radiation from two points lying along the direction of the wave propagation front, interference will be observed if the path difference between the interfering beams is less than the quantity  $c/\Delta v = \lambda^2/\Delta\lambda$ . The quantity  $\Delta_l = (\lambda^2/\Delta\lambda)/\theta_h^2 = (\lambda/\Delta\lambda)\delta/\theta_h$  is consequently the longitudinal dimension of the coherence region, and consequently the required monochromaticity is

$$\frac{\Delta\lambda}{\lambda} < \frac{\delta}{l\theta_h} = \frac{\delta^2}{\lambda l},$$

where  $l$  is the maximum permissible sample thickness (for obtaining a two-dimensional hologram) or the object thickness (for obtaining a three-dimensional hologram).

Note that if instead of the wavelength  $\lambda$  we used the photon momentum  $p$  ( $|\mathbf{p}| = h/\lambda$ ), then the spread in momenta is  $\Delta p_{x,s} = \theta_{x,s} |\mathbf{p}|$ , and the condition of usefulness of the photons is written in the form

$$\Delta_0 \Delta p \leq \hbar$$

for each of the transverse directions, i.e., the photons useful for holography, or, in other words, the mutually coherent photons, will be those passing through a cell of the (transverse-coordinate, transverse-momentum) phase space of area  $\hbar$  ( $\hbar$  is Planck's constant) in each of the transverse directions. Since the "optical" operations with the photons in the region from the source to the subject do not change their phase density, the source will provide a number of useful photons per second

$$\dot{N}_x = \frac{d\dot{N}_x}{d\Omega} \frac{\lambda^2}{\lambda_x \Delta_x} \frac{1}{h^2} \hbar^2 \frac{\Delta\lambda}{\lambda} = B_x \lambda^2 \frac{\Delta\lambda}{\lambda},$$

and the problem is only to use these photons as effectively as possible.

Here, by placing a diaphragm of the necessary size near the source, we can increase the transverse dimensions of the coherence region, keeping the total number of mutually coherent photons unchanged (for the condition, of course, that diffraction at the diaphragm is sufficiently small).

If it is sufficient that  $\Delta\lambda/\lambda \gtrsim 1\%$ , then it is ideal to use a coordinate-sensitive detector with a high efficiency for photon counting and the necessary energy resolution. High-efficiency detectors which have sufficient coordinate resolution and poor energy resolution and detectors which have sufficient energy resolution and which record all photons within some entrance aperture already exist. Indeed, one can imagine detectors produced by means of modern microelectronics which combine the two forms of resolution.

If it is required to go over to  $\Delta\lambda/\lambda$  much better than 1%, the only means apparent at the present time is to use crystal monochromators. The features of using

monochromators have already been discussed in Sec. C of Chap. 2.

The number of resolved elements of the detector should be greater than the number of resolved elements of the sample in each of the directions, and the distance from the detector  $L_2$  should be sufficient that the coordinate resolution  $\delta_{\text{det}}$  is adequate for resolution of the closest maxima,

$$L_2 > \frac{\lambda_0}{\lambda} \delta_{\text{det}}$$

In addition, if the following condition is satisfied,

$$L_2 > \frac{\lambda_0^3}{\lambda},$$

the closest maxima will be completely separated and the reproduction of the image of the object by the hologram reduces to a simple Fourier transformation, for which very efficient and rapid algorithms have been developed.

In order that the interference pattern can be minimally distorted by statistical quantum noise, it is required, roughly speaking, that the intensities of the waves scattered by the illuminator and the sample be close to each other at each point of the hologram. For an arbitrary subject with contrast of the order of unity (for a desired resolution  $\delta$ ) the best approximation to an optimum illuminator will be an aperture of dimension  $\delta$  through which pass (and are diffracted) half of the flux of mutually coherent photons; the remaining photons pass through the sample being studied. Collection of the necessary fraction of the photons into the small aperture evidently can best be accomplished by means of Fresnel zone plates. Here it turns out that the difficulties in preparation of a zone plate which collects an almost parallel photon beam into a size  $\delta$  are of the same nature and order as the difficulties in preparation of an illuminator aperture of size  $\delta$ ; the point is that for this purpose the width of the narrowest (outer) zone of transmission on the plate must be just of this size. Here the optical quality of the zone plate and the illuminator aperture need not be especially high: Their quality determines only the efficiency of utilization of the flux of mutually coherent photons.

An important advantage of holography is the fact that the contrast of a hologram (for optimum choice of reference illumination) does not depend directly on the contrast of the sample and can remain high even for very weakly absorbing and weakly phase-shifting samples. The central part of the transmitted beam carries only a small fraction of the holographic information (regarding the shape of the object) and often it is possible simply not to record this portion. The contrast of the hologram will be reduced only by background scattering in the sample material. In photographing low-contrast samples the problem of collecting the photons into the illuminator is simplified, since the number of diffracted photons from the sample is substantially decreased and a correspondingly smaller flux of photons from the illuminator is required.



If the sample is not purely two-dimensional, then for the same number of resolved elements  $(\Delta_0/\delta)^2$  we can also determine from the hologram the longitudinal position of the elements; here the longitudinal resolution will be  $\delta/\theta_h$ , i. e., substantially poorer than the transverse resolution.

Reproduction of an image of the sample from the hologram, with the photon-counting technique most natural for the x-ray region, is apparently most reasonably accomplished by pure information processing in a computer (with a subsequent synthesis of the image, if necessary). However, it is useful to have in mind that with use of analog detection (see the section on contact microscopy) it is quite possible to reproduce subsequently an enlarged image by means of an ordinary optical laser.

Interesting possibilities are opened up if we make the illuminator structurally similar to the sample being studied. Here the samples can have complicated periodic structures, and accordingly, distinct directions of diffraction. Observation of the interference pattern in this case can provide a representation of the difference between the samples studied and the reference illuminator, and the possibility appears, in particular, of tracing the development of these differences with time. It is possible also to use other variants of illuminators, in particular, a matte illuminator consisting of stochastically placed diffracting details with a size equal to the desired resolution  $\delta$ . These variants obviously have their fields of application. The knowledge of the field of radiation of such illuminators, which is necessary for reproduction of the image of the sample being studied, can be obtained by a single exposure of the sample-illuminator with use as illuminator of an aperture of the necessary size  $\delta$ .

Let us consider an example of the proposed scheme of holographic microscopy<sup>[39]</sup> using as a radiation source the storage ring VEPP-3, whose brightness in the region  $\lambda = 1-2 \text{ \AA}$  is  $B_\lambda \sim 10^{24} \Delta\lambda/\lambda$  (photons/sec-sr-cm<sup>2</sup>).

As a sample studied let us consider an object with contrast of the order of unity in which it is required to distinguish  $n^2 = 50 \times 50$  details. The interference pattern is recorded by a detector with a detection efficiency close to unity (prepared from wire proportional chambers) of size  $20 \times 20 \text{ cm}^2$  and spatial resolution  $1 \times 1 \text{ mm}^2$ . We shall place this detector at a distance of 20 m from the objects.

With use of radiation with  $\lambda = 1 \text{ \AA}$  the detector permits a resolution in the sample  $\delta = 50 \text{ \AA} \times 50 \text{ \AA}$  to be obtained, and a longitudinal resolution of about  $0.25 \mu$ . To provide a statistical accuracy of about  $\sim 10\%$  it is required to record  $\sim 10^6$  photons. For optimal focusing on an illuminator aperture of diameter  $50 \text{ \AA}$  the necessary exposure time is  $T \sim 1 \text{ sec}$  for  $\Delta\lambda/\lambda = 2 \times 10^{-2}$ .

## 5. USE OF SYNCHROTRON RADIATION FOR X-RAY STRUCTURE ANALYSIS

Up to this time we have discussed, so to speak, individual microscopy of a sample, intended to provide

information on the size and location of each individual detail. If we are interested in the characteristics of an entire ensemble of identical or nearly identical objects, then, depending on their relative location, by studying the interaction of x rays with these ensembles we can obtain diverse and sometimes very complete information on the objects of interest.

Depending on the degree of order of the locations of the objects being studied, the diffraction pattern of x rays hitting the objects varies. The kind and amount of information which can be expected from this pattern also varies.

If the objects studied are arranged in the sample completely at random, the diffraction pattern of so-called diffuse scattering from the entire sample will be simply the incoherent superposition of the scattering patterns of the individual objects. In this case it is possible to obtain the distribution pattern of the effective electron density over the object; here the objects may be individual atoms in the gas, density fluctuations in liquid, droplets in an emulsion, and so forth.

With increase of the degree of order of identical objects (fixing of centers, alignment of one of the axes, etc.) the diffraction pattern becomes more and more coherent, with sharp transitions from strongly illuminated regions (reflections) to weakly illuminated ones, and also more and more informative. In this case, however, for highly ordered systems it is necessary in addition to change the orientation of the object with respect to the incident monochromatic radiation, or to use several wavelengths (in the limit, a continuous spectrum) with determination of the photon energy corresponding to each reflection.

In the case of an ideal crystal constructed of completely identical and identically located unit cells, it is possible to determine the location of each atom if it is not too light.

If we assume that the details of interest in the objects have dimensions  $d$ , that the transverse dimensions of the region in which these objects are distributed are  $\Delta$ , and the relative measurement accuracy necessary in a given experiment is  $\delta/d$ , then with radiation of wavelength  $\lambda$ , a spread in the angles of incidence on the object  $\delta\theta$ , and a detector located at a distance  $L$ , the following relations must be satisfied to avoid confusion (we assume  $\lambda/d < 1$ ):

$$\delta\theta < \frac{\lambda}{d} \frac{\delta}{d}, \quad L > \Delta \frac{d^2}{\delta\lambda}.$$

The requirement for monochromaticity (or accuracy in energy detection) is  $\delta\lambda/\lambda < \delta/d$ . Here the angles introduced by the monochromator must be sufficiently small:  $\delta\theta_M < (\lambda/d)\delta/d$ . Since for ordinary monochromators  $\Delta\theta_M \approx \Delta\lambda/\lambda$ , the use of preliminary monochromatization for  $\lambda/d \sim 1$  (diffraction at large angles) will not lead to loss of the useful number of photons. For  $\lambda/d \ll 1$  (small-angle diffraction) it is necessary either to record the photon energy or to accomplish monochromatization directly in front of the detector (which leads to a large additional radiation loading of the object by

unused photons), or to suffer a large loss in the number of useful photons (by  $d/\lambda$  times) (see also Sec. C of Chap. 2).

A very important step would be the creation of monochromators providing at their exit many lines (each of the necessary width) separated by a distance sufficient for reliable resolution by means of coordinate- and energy-sensitive detectors. Such a monochromator corresponds to ordinary monochromators with high efficiency in the higher orders but with a comparatively small distance between lines.

If the number of objects of interest in the sample can be arbitrarily large, then of course it is possible in principle to use the entire radiation of any source (for example, separating the radiation by mirrors and using independent detectors, i.e., performing simultaneously many independent experiments). The limitations of the actually usable flux of photons in this case will be of a technical nature. We shall discuss in somewhat more detail the case in which the number of such objects in the sample is limited. This is characteristic, for example, of protein crystals, which are obtained in sufficiently perfect form only with great difficulty and which therefore have a small volume.

If the two transverse directions in this case have equal standing, then the phase space of the photon flux reaching the sample in one direction should be no greater than

$$\Delta\delta\theta < \Delta \frac{\lambda}{d} \frac{\delta}{d},$$

and correspondingly for optimal focusing the total useful photon flux  $\dot{N}_E$  will be

$$\dot{N}_E \ll B_i \lambda^2 \left(\frac{\lambda}{d}\right)^2 \left(\frac{\delta}{d}\right)^2 \frac{\Delta \lambda}{\lambda}.$$

If the total volume is limited and is small, then in comparison of the useful photon flux from different sources the sample can reasonably be assumed cubic,  $\Delta \sim V^{1/3}$ , where  $V$  is the sample volume.

In comparison with the useful photon flux in microholography the large factor  $(\Delta/d)^2$  corresponds to an increase in the number of objects, and the small factor  $(\delta/d)$  appears as the result of the additional requirements of accuracy in measurement of the characteristic dimensions (and not simply the requirement of resolution, as for a problem in microscopy). The limiting angular resolution determined by diffraction in a dimension  $\Delta$  will be  $\lambda/\Delta$ .

In all types of x-ray diffraction structure analysis the main advantage of using SR is the much higher spectral brightness than in other sources, and the possibility of working with any wavelength. Therefore the greatest gain is obtained if it turns out to be possible to use detectors which simultaneously record both the point of arrival of the photon at the detector and its energy with the necessary resolution.

In studying periodic large-scale molecular structures

such as occur in many biological objects and particularly in muscle fibers, use of SR has decreased the exposure time both as the result of the higher brightness and as the result of selection of the optimal wavelength providing a diffraction pattern with the best intensity and contrast. The requirement of transparency of the objects for the radiation used requires use of sufficiently small  $\lambda$ , and accordingly the diffraction angles in such structures will also be small. It can turn out to be useful to work near the  $K$  absorption edges of any elements occurring in the object, comparing the diffraction patterns on both sides of the  $K$  edge.

Use in such experiments of even presently available high-efficiency detectors of x-ray photons, connected on line with a computer, permits reduction of the exposure time by many orders of magnitude and going over, in particular, to photographs of the dynamics of structural rearrangements of living objects.

Thus, in the first experiments on the rapid study of solutions of biopolymers by the method of small-angle diffuse scattering<sup>[41]</sup> (the technique has been tested in the previously investigated globular albumin pepsinogen) by means of the synchrotron radiation of the VEPP-3 storage ring at our Institute and a one-coordinate proportional chamber developed also at our Institute, it has been shown that in a time  $\sim 100$  sec the scattering curve is obtained with the necessary statistical accuracy. In an x-ray tube with use of the photographic detection method the exposure time was 20–40 hours.

A still greater gain in time, permitting the transition to study of the dynamics of structural rearrangements, was obtained in experiments on small-angle diffraction. In an experiment carried out by workers at the Institute of Biological Physics (Pushchino) and at our Institute on study of the structure of a living frog muscle in the process of contraction, a beam of SR from the SR channel of the VEPP-3 storage ring was reflected from a monochromator ( $\lambda \sim 1-2 \text{ \AA}$ ,  $\Delta\lambda/\lambda \sim 6 \times 10^{-5}$ ) and after necessary diaphragming hit the sample (frog muscle). The diffraction pattern was recorded by means of a single-coordinate proportional detector. The distribution of photons along the coordinate was recorded by a multichannel analyzer whose memory was divided into eight groups of 500 channels each. The information stored in the memory was processed by computer.

Contraction of the muscle was produced by electrical excitation with a special stimulator triggered by pulses from a synchronizing generator. This generator synchronized the operation of the detecting apparatus with the phase of the muscle contraction. The muscle contraction cycle ( $\sim 64$  msec) was broken down into eight time intervals, and information from the detector in each of the intervals was recorded in one of the eight groups of the analyzer memory. This detection system permitted an eight-frame film to be made and permitted the change in the muscle structure to be observed in the various phases of the contraction (Fig. 12). The first experiment was carried out by superposition of the information obtained from 100 muscle contractions. Monitoring of the stability of the muscle contraction in each

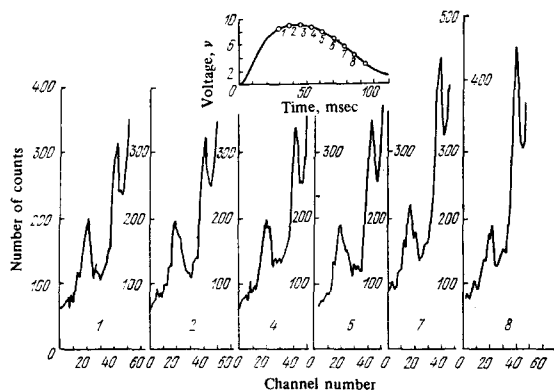


FIG. 12. Equatorial reflections of few-node diffraction patterns of the sartorius muscle of a frog, obtained in the process of stress development. In the upper part of the figure we have shown the times when the diffraction patterns were taken, with a step of 8 msec.

of the 100 cycles was accomplished by means of a strain gauge whose signal was observed on a storage scope.

Increase of the detector speed (it was limited by the analyzer and amounted to 30 kHz) and selection of an arrangement with optimal utilization of the useful quanta (see the discussion on the choice of the location of the monochromator and the focusing) will in the future permit the entire experiment to be carried out in a single contraction.

It frequently is of interest to study the structure at various points of an object, particularly of such non-uniform objects as biological ones. The decrease achieved in the exposure permits this information to be obtained in a reasonable time by placing a diaphragm of the necessary size in front of the object. The limitation in the accuracy of measurement of the periods of the object will be the diffraction at this diaphragm.

It may turn out to be interesting to use coherent illumination of an object (as in x-ray holography). In this case it is possible to record diffraction at extremely small angles. Thus, workers at our Institute, using coherent illumination, have recorded (Fig. 13) the diffraction of x-rays with  $\lambda = 1.8 \text{ \AA}$  from a single slit of size  $d = 4 \mu$  (diffraction angles  $\theta = \lambda/d \sim 4 \times 10^{-5}$ , angular resolution  $\delta\theta \sim 10^{-5}$ ). To obtain a sufficiently large region of spatial coherence, preliminary diaphragming of the SR beam was used. Monochromatization of the radiation was accomplished by a crystal monochromator placed in front of the detector (see Sec. C of Chap. 3), and a total-external-reflection mirror was used to suppress higher order spectra ( $n\lambda = 1.8 \text{ \AA}$ ).

Coherent illumination makes it possible to obtain also an idea of the correlation lengths of a structure, and if two separated diaphragms are used, to obtain in the vicinity of each reflection an interference pattern permitting comparison of the structures of these regions. Obviously this applies also to diffraction patterns at large angles.

In study of the atomic structure of a unit cell (classical x-ray analysis) the use of SR permits the transition

to use of microcrystals (as we have mentioned, this is particularly important for objects such as proteins). A very interesting possibility is that of obtaining diffraction patterns near the *K* absorption edge (more precisely, near the *K* edge on both sides and at some distance) of a heavy atom occurring in the unit cell or specially introduced there. As Herzenberg and Lau<sup>[42]</sup> have shown, by this means it is possible to determine the phase of all reflections and accordingly to establish uniquely the structure of the unit cell of an object of known chemical composition.

Experiments on the use of SR in structural analysis carried out in the VÉPP-3 storage ring by workers from the Kurchatov Atomic Energy Institute and from our Institute<sup>[43]</sup> have shown that the use of synchrotron radiation permits a substantial reduction ( $\sim 100$  times) in the exposure time in the study of protein structure and permits diffraction patterns of a protein crystal of dimensions  $\sim 10^{-3} \text{ mm}^3$  to be obtained in a time of  $\sim 1$  hour (Fig. 14). As a result there is the prospect of studying the structure of protein crystals of volume  $\sim 10^{-4} - 10^{-6} \text{ mm}^3$  and of studying the structures of proteins which do not crystallize readily. The possibility of such experiments became more obvious after the use as a detector of a multiwire chamber operating on line with a computer<sup>[43]</sup> and permitting still greater reduction of the experiment duration, to assure linearity of the measurements over a wide range of reflection intensities and reduce the labor of analyzing the x-ray diffraction pattern.

The high brightness of SR, besides permitting minimum size of the crystals being analyzed, permits nanosecond exposures for large crystals, which can be interesting and even of fundamental importance in analysis of materials under extreme conditions (x-ray structure analysis at explosive pressure, in high pulsed magnetic fields, etc.). Here the low duty cycle of SR turns out to be useful (the nanosecond or shorter duration of the electron bunches for a time of revolution—the time between successive SR pulses—of a fraction of a microsecond or longer). Here it is possible to trace the entire dy-

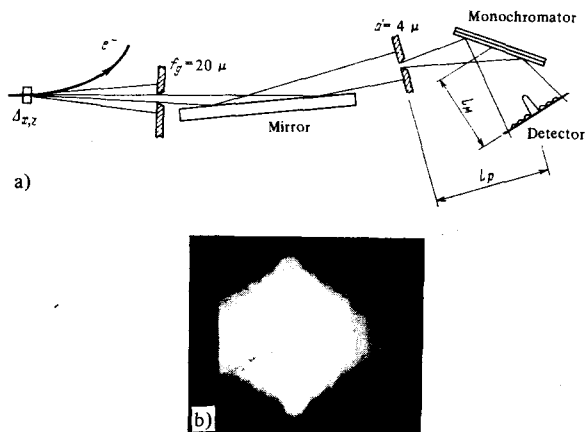


FIG. 13. a) Arrangement for obtaining diffraction of x rays ( $\lambda = 1.8 \text{ \AA}$ ) from a single slit ( $d = 4 \mu$ ); b) photograph of diffraction pattern. The number of maxima is limited by the size of the monochromator used.

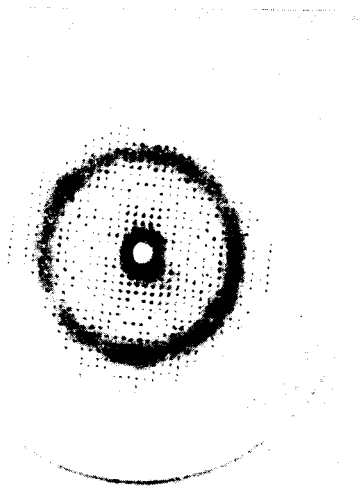


FIG. 14. Precession diffraction photograph of a crystal of the protein AFP (MO-differential).  $\lambda = 1.3 \text{ \AA}$ , exposure time 2 hours, precession angle  $22^\circ$ .<sup>[43]</sup>

namics of the process being studied. In this case the optimum detectors will be parallel ones with scanning, such as image converters.<sup>[44]</sup>

An intermediate situation is occupied by experiments in which the microscopic nature of the objects studied and the shortness of the required exposure are both important at the same time. This situation exists in study of the behavior of materials near phase-transition points, and in particular near crystallization points. Use of the complete SR spectrum obviously provides the possibility of studying extremely small and briefly existing crystalline portions (crystallization of melts, solutions, drops, films, etc.).

## 6. STUDY OF INTERACTION OF RADIATION WITH ATOMS, MOLECULES, AND CONDENSED MATTER

The use of synchrotron radiation has resulted in revolutionary changes in the possibilities of standard experimental methods of determining the electronic structure of matter, based on the study of absorption, reflection, and fluorescence spectra and photoelectron emission. The wide energy range (from 10 eV to 100 keV) permits coverage of the entire region of characteristic atomic energies high than laser energies.

The increase of the source brightness by several orders of magnitude makes it possible to carry out these experiments in a short time and with high energy resolution (the source brightness is particularly important if preliminary monochromatization is required). The natural polarization of the radiation permits study of the spatial anisotropy of objects (crystals, oriented molecules).

The time modulation of synchrotron radiation (the short pulse, the known distribution of the light pulse, and the high repeatability of the pulse arrival) permits study of time characteristics of luminescence and measurement of the energy of photoelectrons ( $h\nu \sim 1\text{--}100 \text{ eV}$ ) from their time of flight.

Synchrotron radiation is already turning out to be useful in study of atomic form factors for elastic scattering, which are important for quantitative x-ray structure analysis. However, the usefulness of SR appears much more clearly in study of the structure of the  $K$ ,  $L$ , etc., absorption edges. With the high resolution achievable with bright sources, this structure turns out to be very rich and provides information on the energy spectrum of isolated, noninteracting molecules in which the atom studied occurs, and on the detailed effects of interatomic interaction.

Thus, investigation of the change in the absorption coefficient for x rays at energies 100–1000 eV above the  $K$  edge of the atom studied permits determination of the distance between the atoms surrounding the absorbing atom.<sup>[45]</sup> This method, extended x-ray absorption fine structure (EXAFS), which is widely used in the SR beams at SPEAR, has been applied to a large class of objects (gases, liquids, crystals, glasses, proteins). It has been shown experimentally that the accuracy in determination of the distance between atoms is  $\pm 0.05 \text{ \AA}$ . This method acquires special value in study of the local surroundings of specific metal atoms in proteins which provides the possibility of understanding the role of such atoms in biological processes.

As a result of the high intensity of SR sources it is possible to obtain the limiting degree of monochromatization possible for existing monochromators. The greatest interest in use of such radiation is in studies of those atomic transitions in molecules which have a comparatively small width of the intrinsic level.

In the vacuum ultraviolet region ( $\lambda = 300\text{--}3000 \text{ \AA}$ ) the very best resolution at the present time ( $\Delta\lambda = 0.03 \text{ \AA}$ ) is apparently obtained in the three-meter monochromator installed in the SR beam of DORIS.<sup>[30]</sup> This monochromator permits measurement of the shape of lines of the autoionization series and the intensities of the rotational and vibrational levels of simple molecules (Fig. 15). The monochromator in combination with an electron kinetic-energy analyzer can be used to study the photoemission threshold.

A limiting resolution  $\Delta\lambda = 0.04 \text{ \AA}$  in the region  $\lambda = 80\text{--}20 \text{ \AA}$  has been obtained in the VEPP-2M storage ring by a group from the Institute of Inorganic Chemistry at Novosibirsk. Figure 16 shows the absorption spectrum of sulfur in the  $\text{SO}_2$  molecule. In addition to the well

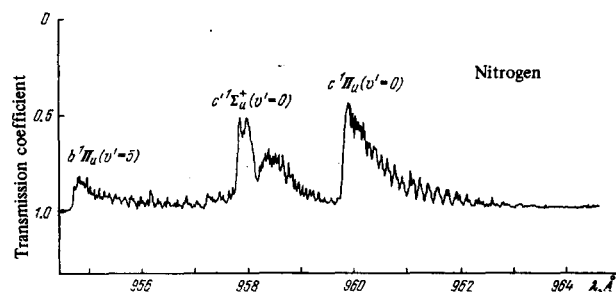


FIG. 15. Absorption spectrum of  $\text{N}_2$ , demonstrating the existence of three vibrational levels in the vicinity of  $960 \text{ \AA}$ .<sup>[30]</sup>

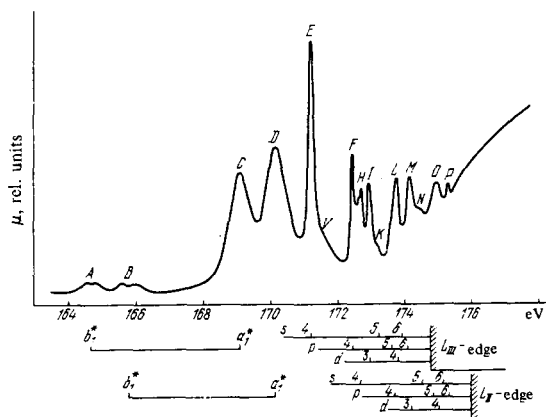


FIG. 16. Absorption spectrum of the  $\text{SO}_2$  molecule in the region of the  $L_{II-III}$  absorption edge of sulfur.<sup>[46]</sup>

resolved structure of the Rydberg series the fine structure of the first  $L_{II-III}$  absorption bands has been distinguished.<sup>[46]</sup> On the basis of such spectra for systems of two or three atoms which are fragments of complex chemical compounds, it is possible to study various chemical interaction effects. Here the materials studied can be taken either in the form of a vapor or in the form of molecular, atomic, or ionic beams.

Data on the interaction with atoms of photons with energy well above the ionization energy may turn out to be very interesting (the study of collective excitations). Gadiyak *et al.*<sup>[47]</sup> predict the existence of such excitations (dipole oscillations of a shell as a whole with respect to the nucleus) at energies  $h\nu_1 = 13.7Z$  eV and  $h\nu_2 = 36.0Z$  eV ( $Z$  is the atomic number of the element) with energy widths  $\Gamma_1 = 3 \times 10^{-3}Z$  eV and  $\Gamma_2 = 10^{-4}Z$  eV. The search for such narrow resonances in multielectron atoms (and perhaps also in condensed media) may be interesting also from the point of view of study of the possibility of making x-ray lasers.

The high intensity of SR in the x-ray region makes it possible on the basis of luminescence spectra, studying the intensities and energy locations of lines due to transitions from high levels after photoionization of one of the lower levels, to obtain information on the chemical state of rather heavy elements in a condensed medium at very low concentrations and for very short periods of time. In particular, this permits analysis of the chemical state of catalysts under various conditions and in different stages of a reaction.

The use of synchrotron radiation from the VÉPP-3 storage ring to excite the emission spectra of highly disperse nickel, carried out by scientists from the Institute of Catalysis at Novosibirsk,<sup>[48]</sup> has made it possible as the result of the high intensity of the SR to greatly reduce the exposure time (for example, the weakest line of the spectrum,  $K\beta_5$ , from a sample containing 1% Ni was obtained in 1.5 hours). Measurements of the shape and energy location of the lines  $K\beta_1\beta'$  and  $K\beta_5$  and also of the splitting of the  $K\beta_1\beta'$  multiplet as a function of the size of the Ni particles have permitted the elec-

tronic structure of the disperse systems to be recorded as a function of the size of the particles and have revealed a substantial change in the electronic structure for Ni particle sizes less than 10 Å.

Recently synchrotron radiation has been used extensively to investigate the excitation mechanism of luminescence in the vacuum ultraviolet region.<sup>[18,23]</sup> Recently new results were obtained in studies carried out by a group from Moscow State University at the VÉPP-3 storage ring,<sup>[58]</sup> on the luminescence of various crystals ( $\text{BeO}$ ,  $\text{MgO}$ ,  $\text{Y}_2\text{O}_3$ ) on excitation of the crystals by intense x rays in synchrotron radiation. The intense peaks observed in the luminescence spectra in the region  $h\nu \sim 5-7$  eV present substantial interest from the point of view of the possibility of using these crystals as the materials for vacuum ultraviolet lasers, efficient transformation of x-ray energy in x-ray phosphors, and so forth.

## 7. USE OF SYNCHROTRON RADIATION TO DETERMINE THE CHEMICAL COMPOSITION OF OBJECTS

Investigation of the emission spectra of characteristic x rays is the classical method of studying the electronic structure of a material. In addition, x-ray fluorescence analysis is being widely used at the present time in a number of purely practical applications to determine the chemical composition of various objects, including biological objects.<sup>[49]</sup> The characteristic radiation is usually excited by x-ray tubes, radioactive isotopes, or beams of charged particles. The detectors are either spectrographs which decompose the radiation by wavelength or semiconductor detectors which have good energy resolution ( $\sim 130$  eV at  $h\nu \sim 6$  keV).

The use of synchrotron radiation to excite fluorescence permits reduction of the time required for the experiments and of the radiation exposure of the sample, and also increase of the sensitivity due to the substantial reduction in the background determined by coherent and Compton scattering of the primary photons in the sample.

In experiments of this type it is convenient to select from the SR spectrum a portion of width several percent with a lower limit somewhat above the working absorption edge. In the x-ray region this can be achieved by a combination of total external reflection (removal of the short-wavelength part) and properly selected absorbers. It is also possible to use for this purpose high-aperture crystal monochromators of graphite, which provide  $\Delta\lambda/\lambda \sim (1-5) \times 10^{-2}$ .

In this case in the primary flux there are no photons with the energy of the characteristic radiation, which completely removes the background due to coherent scattering when the detector is a semiconductor detector with energy resolution much better than the interval between the lower edge of the incident-radiation spectrum and the energy of the characteristic photons.

The natural linear polarization of SR leads to an angular anisotropy in Compton scattering, since the cross

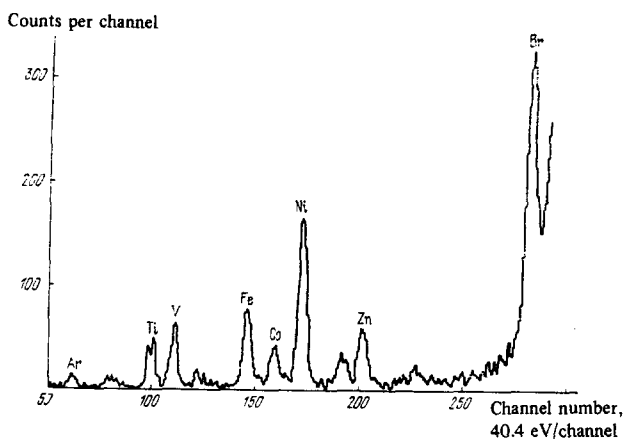


FIG. 17. Fluorescence spectrum of petroleum excited by synchrotron radiation.<sup>[50]</sup>

section for Compton scattering in the nonrelativistic case is

$$d\sigma = \left(\frac{e^2}{mc^2}\right)^2 \sin^2\theta d\Omega,$$

where  $\theta$  is the angle between the direction of scattering and the direction of the electric field of the incident wave. The degree of linear polarization of the radiation falling on the sample can be made practically 100% with use of monochromators with Bragg angles close to  $45^\circ$ .

By using linearly polarized radiation for excitation of fluorescence, placing the detector at an angle  $\theta = 0$ , and decreasing the detector solid angle and the spot size at the sample, it is possible to reduce greatly the background determined by Compton scattering. In this case the background due to single Bragg reflection from possible crystalline inclusions also decreases.

The sensitivity of the method can be increased (with loss of speed) if use is made of a narrow spectral interval (less than the width of the absorption edge) of the incident radiation and if repeated comparison is made of the energy spectrum of the scattered radiation on excitation just below and just above the absorption edge. This method also gives the least radiation dose to the sample studied.

Workers from our Institute, from the Institute of Geology and Geophysics and the Institute of Inorganic Chemistry of the Siberian Division of the USSR Academy of Sciences, and from the Institute of Biological Physics of the USSR Academy of Sciences have carried out experiments to determine the chemical composition of various objects (salt solutions, petroleum, powdered minerals) with SR from the VEPP-3 accelerator.

The excitation was carried out with monochromatized radiation with  $\Delta\lambda/\lambda \sim 3 \times 10^{-2}$  at a wavelength close to the  $K$  edge of the element investigated. The detector was a Si(Li) semiconductor detector made by ORTEC, placed at right angles to the SR beam direction. A special collimator system separated fluorescence radiation coming from the sample in a comparatively small solid angle near the direction of the polarization vector of the incident synchrotron radiation.

Under these conditions it was possible to obtain a sensitivity which is evidently the best obtained for fluorescence analysis (for example, the presence in water solution of Zn with a concentration  $\sim (2-3) \times 10^{-8}$  g/g is easily observed). The time necessary for an exposure was  $\sim 100$  sec for a concentration of  $10^{-7}$  g/g. In Fig. 17 we have shown a fluorescence radiation spectrum of petroleum.

Of course, the use of synchrotron radiation for routine chemical analysis is not justified at present, if only because of the limited number of synchrotron radiation sources. However, in unique experiments (the search for superheavy elements,<sup>[51]</sup> the analysis of lunar rock, and so forth) the use of synchrotron radiation may be extremely effective.

## 8. NUCLEAR SPECTROSCOPY AND RELATED QUESTIONS<sup>2)</sup>

The spectral density of the flux of SR photons is so high that within the characteristic widths of nuclear levels strongly coupled by electromagnetic transitions with the ground state an object can receive a rather intense flux of well collimated photons. Thus, within the width of the  $\text{Re}^{187}$  level at  $E = 134$  keV,  $\Gamma = 4.6 \times 10^{-5}$  eV, in the storage rings VEPP-4, PEP, and PETRA it is possible to obtain  $10^5 - 10^6$  photons/sec in a solid angle of  $10^{-4} \times 10^{-3}$  sr. The use of wigglers can raise the intensity by another two orders of magnitude. The building of such storage rings will permit coverage of the entire range of photon energies characteristic of nuclear transitions. The time and polarization structure of SR present new possibilities for nuclear spectroscopy.

Ordinary monochromatization by means of perfect crystals permits separation of photons exciting any single level (the distance between different levels is much greater than the energy spread given by a good monochromator). The combined use of the best possible monochromatization of the incident radiation, energy discrimination in detection of the scattered photons, and use of photons scattered into the backward hemisphere will permit the greatest possible reduction of the background due to electron scattering. In this case it is possible to study not only nuclear scattering, but also to see the entire cascade of decays from an excited state. It is particularly convenient to use SR for study of metastable levels (for example, measurement of the magnetic moments of excited states, the search for transitions suitable for creation of  $\gamma$ -ray lasers, etc.).

New possibilities are opened up for Mössbauer experiments with use of the radiation of narrow nuclear levels populated by means of synchrotron radiation. Here it is possible to populate Mössbauer levels through wide levels with energy  $E_0 > 100$  keV coupled by strong electromagnetic transitions both with the ground state and with the interesting Mössbauer level with energy  $E_M$ . This question has been partially discussed by Dmitriev and Shuryak.<sup>[51]</sup> An advantage of this means

<sup>2)</sup>This section was written jointly with M. I. Shtokman.

of producing Mössbauer radiators is the possibility of including a much larger group of nuclei and the complete absence of residual activity after turning off the SR beam.

The fraction of primary absorption events for photons with energy  $E_M$  which give useful Mössbauer photons emitted in the total solid angle is determined by the relative probabilities of a transition from the level  $E_0$  to the level  $E_M$ , of a radiative transition from the level  $E_M$  to the ground state, and of the Mössbauer effect in a given medium at a given temperature. The lifetime of a Mössbauer level is much greater than the relaxation time of the recoil nucleus after absorption and radiation of high energy photons, so that no further decrease in the number of useful photons occurs.

In order that the flux of Mössbauer photons not be attenuated as the result of nuclear absorption, the primary photons must be absorbed in a thin surface layer of the material used and correspondingly the angle between the direction of incidence of the primary photons and the absorbing surface must be no greater than  $\sigma_{E_0}/\sigma_{E_M} \approx (E_M/E_0)^2$  ( $\sigma_{E_0}$  and  $\sigma_{E_M}$  are the cross sections for interaction of the corresponding resonance photons).

To decrease the flux of parasitic photons accompanying the necessary Mössbauer photons, the thickness of the Mössbauer radiator is conveniently made close to the thickness of nuclear interaction of the photons, by making the emitter in the form of a film on a light substrate. For the same purpose it is reasonable to make the spectrum of the incident radiation with energy  $E_0$  hitting the emitter as narrow as possible by means of a perfect monochromator crystal (it is true that the width of the spectrum will anyway turn out to be significantly greater than the width of any nuclear level). The reflection from the crystal monochromator must be carried out in the vertical plane, placing the monochromator at a distance  $L = \Delta_e/(\delta E/E_0)_M$  from the storage ring ( $\Delta_e$  is the size of the electron beam in the storage ring and  $(\delta E/E_0)_M$  is the energy resolution of the crystal monochromator). For complete utilization of the SR photon flux it is necessary to use a curved crystal.

In detecting the photons which have passed through the object being studied, to reduce the background it is necessary to carry out the best possible energy discrimination, selecting only photons with energy close to  $E_M$  (we recall that the energy resolution of modern semiconductor detectors is better than 1%). In addition, it is useful to utilize time selection in cases when the length of the burst of the radiating electrons and the time resolution of the detecting apparatus are significantly less than the lifetime of the Mössbauer level, selecting only events delayed with respect to the time of passage of the electron burst.

An attractive idea is to obtain by means of SR intense narrowly directed beams of Mössbauer photons. A possible arrangement consists of Bragg reflection from a crystal monochromator (similar to the usual monochromatization scheme) which must contain nuclei of a Mössbauer isotope. Here the crystallinity of the structure and the presence of the Mössbauer effect are nec-

essary to retain the directivity of the photon flux, while the resonant nature of the nuclear scattering and the use of a thin crystal assure preferential reflection of useful photons.

A physical picture of "nuclear Bragg monochromatization" appears as follows. Synchrotron radiation hits a crystal in the form of very short bursts ( $t_{\text{burst}} \sim mc/eH\gamma^2 \leq 10^{-20}$  sec) radiated without correlation by individual electrons. As a result of the periodic location of the nuclei in the crystal they are excited by these pulses with a regular shift in phase. Mössbauer scattering processes (elastic, without recoil) of resonance photons by different nuclei of the crystal are indistinguishable and the corresponding amplitudes add. They interfere constructively at the Bragg angles (if the radiation falls on the crystal at these angles). If the crystal thickness is no greater than the depth of penetration of resonance photons corresponding to the Mössbauer scattering peak, then in the spectrum of a beam deflected in a given direction there will be a narrow, high band of Mössbauer photons (with a width of the order of the width of the corresponding nuclear level) and a significantly lower but much wider band of electron-scattered photons. At this stage of monochromatization it is reasonable to strive for the maximum reduction of the level of electron scattering with as complete as possible preservation of the resonance photons, and to carry out the best possible narrowing of the spectrum of electron-scattered photons beforehand (as described above).

If the crystal thickness is greater than the depth of penetration of the resonance photons, the spectral width of nuclear-scattered photons will be substantially greater (see for example Artem'ev *et al.*).<sup>[53]</sup>

We note that as a consequence of constructive interference the elastic scattering of resonance photons in a "nuclear" crystal is coherently enhanced and becomes of the order of, and in special situations even greater than, the inelastic scattering.<sup>[54]</sup>

The depth of nuclear interaction of Mössbauer photons is very small—only hundreds or thousands of crystal layers, so that a nuclear crystal monochromator must evidently be a thin perfect crystal film containing the necessary nuclei on a substrate of another structure. Here the ratio of the spectral densities of the Mössbauer and electronic components of the deflected beam will be of the order of the ratio of the cross section for Mössbauer scattering to the cross section for coherent electron scattering. For crystals with a high probability of the Mössbauer effect and a high concentration of the necessary isotope, this quantity is much greater than unity. If it is necessary to reduce further the number of background electron-scattered photons, several such reflections can be carried out.

The ratio of the spectral densities in individual cases can be improved if the difference between the electronic and nuclear lattices of the crystal monochromator is utilized. For example, the electronic component will be substantially suppressed if the period of the nuclear scatterers is an integral number of times greater than the period of the electronic lattice. Such a structure

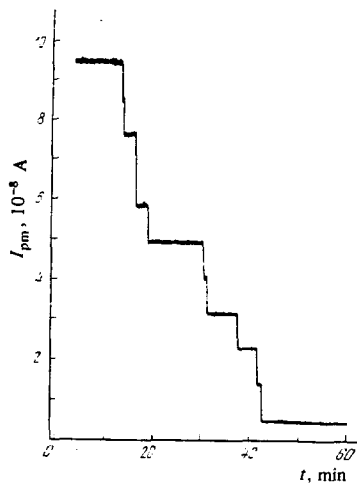


FIG. 18. Time dependence of signal height at the detector recording x-ray synchrotron radiation from several electrons in orbit in the VEPP-3 storage ring. The smallest intensity jump corresponds to the loss of one electron.

can be achieved in principle by several means with different degrees of universality, complexity, and efficiency.

It is also possible to carry out the final stage of Mössbauer monochromatization by using total external reflection from thin films containing the appropriate isotope.

As we have mentioned, in the problem of separating resonance photons in a background of electron-scattered photons, it is very important to make use of the radically different luminescence decay times in detection of the photons. In addition, it may be possible to create fast acting periodic crystal gates which can be placed after a nuclear monochromator to cut out the electron-scattered photons in well collimated fluxes.

The methods described above for obtaining Mössbauer photons provide the possibility of carrying out Mössbauer experiments not only by reflection, but also by transmission. Further improvement of the background conditions can be obtained if we detect photons scattered by the object under study at large angles (this is especially effective for high photon energies): Here the coherent electronic scattering in the object is further suppressed, and the Compton-scattered and luminescence photons can be cut out by comparatively deep discrimination in energy.

The use of SR will evidently permit Mössbauer experiments (all known ones, and possibly also completely new ones) with any nuclei having levels of appropriate energy and width, with limitations imposed only by the specific nature of the Mössbauer effect.

## 9. PROSPECTIVE APPLICATIONS OF SYNCHROTRON RADIATION

The wide range of experiments with synchrotron radiation in the fields of physics, chemistry, and biology permits us now to begin work on use of SR in metrology, medicine, and materials studies and to begin development of new technologies based on SR.

### A. Metrology

The precisely calculable characteristics of synchrotron radiation permit its use as a standard source for

calibration of secondary standards (gas-discharge lamps, x-ray tubes) in the vacuum ultraviolet and x-ray regions. To obtain the best possible accuracy it is necessary to:

- work with a small number of electrons in a storage ring, where each of them can be considered individually (Fig. 18) or with currents  $\geq 10$  mA where the current can be measured with an accuracy of  $10^{-4}$  or better with good lifetime;

- know the energy of the electrons, measuring it, for example, by the method described in Ref. 55;

- have an SR channel with large aperture which does not limit the vertical size of the SR beam.

In addition to absolute calibration of radiation sources, the use of synchrotron radiation permits:

- standardization of radiation detectors in the vacuum ultraviolet and x-ray region;

- calibration of filters and special apparatus (polarimeters, monochromators) for extra-atmospheric astronomy;

- calibration of dosimetric apparatus;

- measurement of the absolute sensitivity of photosensitive materials for detection of radiation over a wide range of the spectrum.

### B. Medical applications

The spectral density of synchrotron radiation in the x-ray portion of the spectrum (2–100 keV) is six orders of magnitude higher than in bremsstrahlung and three orders higher than the characteristic radiation of the best x-ray tubes. Therefore we should expect that synchrotron radiation will find interesting applications in medicine for purposes of diagnostics and radiation therapy, as the result of separating from the SR spectrum a rather intense flux of photons of many wavelengths.

In combination with x-ray proportional detectors<sup>[43]</sup> such use of SR provides the possibility, with a reduction of the radiation dose to human subjects by about  $10^2$ – $10^3$  times in comparison with ordinary x-ray fluorography, of carrying out the following investigations:

- study of the distribution of chemical elements in the human body and its organs and accurate measurement of the variations in concentrations of elements in various types of illness;

- obtaining x-ray photographs of various human organs by working at the *K* absorption edge of an element having increased concentration in a given organ (for example, an x-ray photograph of the circulatory system or the thyroid gland taken at the *K* edge of iodine);

- early diagnosis of new growth of malignant tumors on the basis of the change in concentration of the elements in various organs.

These studies are close to the problems discussed in Chaps. 4 and 8. However, the human body is strongly absorbing for the wavelengths which must be used in study of the distribution of intermediate and light elements. Therefore, of the entire range of interaction



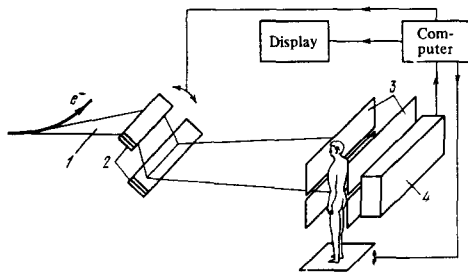


FIG. 19. Possible arrangement for carrying out medical studies by means of synchrotron radiation. 1—SR beam, 2—double-crystal monochromator, 3—diaphragm, 4—one-coordinate proportional chamber.

effects of radiation with the corresponding atoms it is most reasonable to measure the absorption coefficient of radiation at various wavelengths as a function of the spatial coordinate.

In Fig. 19 we have shown a possible arrangement for carrying out medical studies. The arrangement uses apparatus already in use in x-ray structure studies and x-ray spectral experiments with SR.<sup>[32,33]</sup>

A wavelength near the  $K$  absorption edge of the chemical element of interest is selected from the SR beam (1) by means of a double-crystal monochromator (2). For such investigations the SR beam must have a sufficient width (10–60 cm) to provide immediately the distribution of the concentration of the chemical element along the  $x$  axis with use of a one-coordinate proportional detector<sup>[41]</sup> (working length 600 mm, spatial resolution 0.2 mm) and to provide a two-dimensional pattern by moving (scanning) the platform on which the patient stands. The size of the diaphragm (3) placed in front of the patient is chosen as 0.1–1 mm, depending on the required spatial resolution. To improve the background conditions and accordingly increase the sensitivity of the method, it is advantageous to collimate also the transmitted radiation. In addition, it is helpful to use a survey at two wavelengths (exactly at the absorption edge and slightly below the  $K$  edge). Subtraction of the pictures obtained for the different wavelengths also permits increased sensitivity in determination of the concentration of a given element.

Computers can be used to process the information obtained from the one-coordinate detector, and to control the monochromator and also the mechanism for moving the table. The results of the measurements can be presented in a graphic display in an easily understood form.

If a resolution of 1–2 mm is sufficient, it is possible to use two-coordinate detectors, which permits a picture to be obtained immediately without scanning. It will be possible if one can successfully increase the rate of recording of information in comparison with existing systems. In addition, the SR beam must be increased in height to the necessary size (using, say, an exit crystal with an inclined cut in the monochromator).

For problems where it is required to determine very small concentrations of the interesting elements, it is necessary to turn to detectors with high energy resolu-

tion (in this case it is possible to reduce the background by separating the primary radiation from luminescence and Compton photons). Present-day semiconductor detectors which have good energy resolution do not have coordinate resolution. Therefore when they are used it is necessary to use two-dimensional scanning with simultaneous collimation of the incident and transmitted radiation.

We must also point out the possibility of using SR for radiation therapy. In the case where a natural or specially arranged accumulation of a heavy element (with  $K$  absorption edge  $\geq 30$  keV) is possible in a malignant tumor, irradiation by photons with energy just above the  $K$  edge of this element, for a sufficient concentration of the element, obviously permits irradiation only of the diseased tissue in the vicinity of the tumor.

### C. X-ray lithography

In industrial processes for production of modern semiconductor devices (large-scale integrated circuits, microprocessors, etc.) lithography is extensively used to obtain images of some mask on the surface of crystals. Use of lasers permits working with masks having a minimal line thickness 2–10  $\mu$ . This value is determined by the diffraction spreading of the line. To obtain resolution better than 1  $\mu$  it is necessary to have shorter wavelengths, and therefore for this purpose electron beams or x rays are used. X-ray lithography has a number of economic and technological advantages over lithography with electron beams, but the low brightness of x-ray tubes did not make it possible to use lithography in industrial technology, since the exposure time to obtain one image was 1–10 hours with the best x-ray tubes.

Recently<sup>[56]</sup> IBM carried out a systematic study of the use of synchrotron radiation for x-ray lithography. The work was performed in the DESY synchrotron, whose SR has a brightness which permitted exposures from 1 to 100 sec; the spatial resolution obtained was as low as  $5 \times 10^{-2}$   $\mu$  (Fig. 20), and a mask with line thickness  $\leq 1$   $\mu$  is easily reproduced at a mask-crystal distance of 1–2 mm. Various technological materials were studied, and it was shown that up to  $10^4$  images can be obtained from one mask without loss of resolution. From the study it was concluded that an electron storage ring with energy 0.6–1 GeV and a cost of about one million dollars is an ideal source for x-ray lithography and can be used directly in industrial production.

It is entirely possible that introduction of the new technology may lead to creation of a new generation of contemporary semiconductor devices.

### D. Molecular microsurgery

The high spectral density of SR and the possibility of separating any wavelength in the range 0.1– $10^3$   $\text{\AA}$  permits use of synchrotron radiation for "surgical operations" in individual molecules.

It is well known that use of ultraviolet radiation from a hydrogen lamp for ionization of organic molecules permits the unambiguous division of molecules into rather large fragments, instead of the large number of

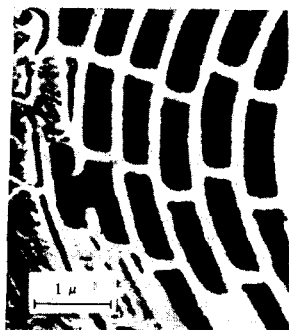


FIG. 20. Replica of a Fresnel zone plate obtained by x-ray lithography. The smallest line thickness resolved in the replica is  $\sim 0.07 \mu$ .<sup>[56]</sup>

small fragments obtained in ionization by an electron beam. This situation is extremely important for the mass-spectrometric method of determining the structure of molecules.

If synchrotron radiation is used for the ionization, it is possible by varying the wavelength to change the place of separation of the molecule and to obtain breakup of molecules into other large parts. This permits a simple and unique determination of the structure of the initial molecule.

Great interest is obviously presented also by the possibility of using synchrotron radiation to cut out previously selected point regions of chromosomes (say, one or several genes), without damaging the whole cell and without destroying the division apparatus.

One of the means of carrying out operations of this type involves the possibility of obtaining microbeams (of diameter  $0.1-1 \mu$ ) of x-ray synchrotron radiation with  $\lambda \sim 10-100 \text{ \AA}$ , which is strongly absorbed in cells (the laser beams used at the present time have a minimum size of  $2-10 \mu$ ). By means of these microbeams it is possible under a microscope to cut out definite portions of cells.

Another possibility is use of monochromatized synchrotron radiation near the *K* absorption edge of intermediate and heavy elements ( $\lambda \sim 0.5-3 \text{ \AA}$ ). In this case one irradiates an entire biological object or an interesting region, but radiation is absorbed only in the region of location of the corresponding atom (which, of course, can be introduced artificially into definite locations of biological molecules). This leads also to the local destruction of individual portions chosen beforehand, or to breakup of molecules in definite places.

Work of this type with use of SR has already begun in Canada.<sup>[57]</sup> One can hope that these microsurgical operations may turn out to be useful in solution of various problems in genetics.

### E. Radiation technology

At first glance it appears that use of SR in radiation-chemistry manufacturing processes cannot become economically justified. However, this situation may change. The point is that the depth of penetration in a light material of photons with energy of the order of  $1-2 \text{ MeV}$  (about  $10-20 \text{ cm}$  of condensed matter with  $Z \sim 15$ ) is the same as for electrons with energy an order of magnitude higher. And at that energy the electrons already produce intense activation of the bombarded objects.

Nonactivating radiation with this penetrating ability is necessary if one wishes to carry out radiation-chemistry industrial processes (such as polymerization) immediately in large prepared objects or in the transition to large-tonnage production where the largest possible penetration depths are also required.

An electron or positron storage ring of energy  $50-100 \text{ GeV}$  can become a highly efficient generator of SR of the necessary region. With use of superconducting resonators such a storage ring can provide megawatts of x rays with a power efficiency close to  $100\%$ . The possibility of having a low duty cycle of the radiation (peak power  $10^3-10^5$  times the average power) also is attractive for radiation processes. The irradiated material can serve as the heat carrier providing transport of the radiated power from SR catchers made of light (nonabsorbing) material and located around the entire perimeter of the storage ring.

The large size of this complex—a perimeter of several kilometers—corresponds completely to the scales of modern chemical and oil refining installations.

Such a storage ring would simultaneously be an installation with colliding electron-positron beams with energy about  $2 \times 100 \text{ GeV}$ , whose value for future elementary-particle physics cannot over-estimated.

## 10. CONCLUSION

In one review it is impossible even to mention all of the published studies with synchrotron radiation carried out in the various centers of the USSR, USA, West Germany, France, England, and other countries. We have only attempted to reveal the research and technological potential of modern synchrotron radiation sources. We have used as illustrations mainly studies carried out in the SR beams of the storage rings of our Institute, and the authors express their gratitude to the staff who have contributed to the performance and evaluation of these studies. The authors also are grateful to their colleagues of the Kurchatov Atomic Energy Institute, the Institute of Physics Problems and the Institute of Biological Physics of the USSR Academy of Sciences, the Institute of Inorganic Chemistry, the Institute of Catalysis, the Institute of Automation and Electrometry, and the Institute of Geology and Geophysics of the Siberian Division, USSR Academy of Sciences, Moscow State University, and the Institute of Catalysis of the USSR Academy of Sciences for their joint work and for useful discussions. The authors particularly express their indebtedness to G. I. Budker.

## APPENDIX

a) The universal spectral function for a section of trajectory with a uniform field is

$$\eta\left(\frac{\lambda}{\lambda_c}\right) = \frac{\lambda_c}{\lambda} \int_{\lambda_c/\lambda}^{\infty} K_{5/3}(x) dx,$$

where  $K_\nu(x)$  is a modified Bessel function of second order (the MacDonald function).

b) The universal spectral function for a wiggler with a field  $H = H_m \cos(\pi s/d)$  is

$$\eta_{wi} \left( \frac{\lambda}{\lambda_m} \right) = \frac{1}{\pi^2} \int_0^\pi d\alpha \int_{1/\sqrt{\cos \alpha}}^\infty K_{5/3}(z) dz,$$

where

$$\lambda_m (\text{\AA}) = \frac{186}{E^2 (\text{GeV}) H_m (\text{kOe})}, \quad y = \frac{\lambda}{\lambda_m}, \quad \alpha = \frac{\pi s}{d}.$$

c) The universal angular function  $\xi = \psi_\lambda / \psi_{\lambda,c}$  was determined by calculation of the angular distribution of the photon flux at various  $\lambda$ :

$$\dot{N}(\lambda, \psi) = 1.33 \cdot 10^{18} \left( \frac{\lambda_c}{\lambda} \right)^2 \frac{\Delta \lambda}{\lambda} E^2 (\text{GeV}) I (\text{A}) \times [1 + (\gamma\psi)^2] \left[ K_{2/3}^2(\beta) + \frac{(\gamma\psi)^3}{1 + (\gamma\psi)^3} K_{1/3}^2(\beta) \right],$$

where

$$\beta = \frac{\lambda_c}{2\lambda} [1 + (\gamma\psi)^2]^{3/2}.$$

d) The average linear polarization is

$$\bar{p} \left( \frac{\lambda}{\lambda_c} \right) = \frac{(\lambda_c/\lambda) K_{2/3}(\lambda_c/\lambda)}{\eta(\lambda_c/\lambda)}.$$

<sup>1</sup>G. Schott, *Electromagnetic Radiation*, Cambridge, Univ. Press, 1912.

<sup>2</sup>I. Ya. Pomeranchuk, *Zh. Eksp. Teor. Fiz.* **9**, 915 (1939).

<sup>3</sup>D. D. Ivanenko and I. Ya. Pomeranchuk, *Dokl. Akad. Nauk SSSR* **44**, 343 (1944).

<sup>4</sup>J. Schwinger, *Phys. Rev.* **70**, 798 (1946).

<sup>5</sup>L. A. Artsimovich and I. Ya. Pomeranchuk, *Zh. Eksp. Teor. Fiz.* **16**, 379 (1946).

<sup>6</sup>D. D. Ivanenko and A. A. Sokolov, *Dokl. Akad. Nauk SSSR* **59**, 1551 (1948).

<sup>7</sup>J. Schwinger, *Phys. Rev.* **75**, 1912 (1949).

<sup>8</sup>A. A. Sokolov and I. M. Ternov, *Zh. Eksp. Teor. Fiz.* **31**, 473 (1956) [*Sov. Phys. JETP* **4**, 396 (1957)].

<sup>9</sup>L. D. Landau and E. M. Lifshitz, *Teoriya polya (Theory of Fields)* Moscow, Gostekhizdat, 1961 [Pergamon, 1965].

<sup>10</sup>J. D. Jackson, *Classical Electrodynamics*, Wiley, 1962. Russ. transl., Moscow, Mir, 1965.

<sup>11</sup>A. A. Sokolov and I. M. Ternov, *Synchrotron Radiation*, Oxford, Pergamon Press, 1968.

<sup>12</sup>V. N. Baier, V. M. Katkov, and V. S. Fadin, *Izlučenje relyativistskikh elektronov (Radiation of Relativistic Electrons)*, Moscow, Atomizdat, 1973.

<sup>13</sup>D. Tomboulion and P. Hartman, *Phys. Rev.* **102**, 1423 (1956).

<sup>14</sup>O. Kulikov, *Trudy FIAN SSSR* **80**, 3 (1975) [Proceedings of the Lebedev Institute].

<sup>15</sup>*Sinkhrotronnoe izlučenje v issledovanii tverdykh tel (Synchrotron Radiation in the Study of Solids)*, Moscow, Mir, 1970.

<sup>16</sup>S. P. Kapitza, a) *Priroda*, No. 10, 22 (1971); b) in: *Proc. of Ninth Intern. Accelerators Conference at SLAC, Stanford*, 1974, p. 671.

<sup>17</sup>*Research Applications of Synchrotron Radiation (BNL 50381)*. Ed. R. Watson and M. L. Perlman, 1973.

<sup>18</sup>*Vacuum Ultraviolet Radiation Physics*, Ed. E. Koch, R. Haensel, and C. Kunz, No. 9, N. Y., Pergamon Press, 1974.

<sup>19</sup>D. F. Alferov, Yu. A. Bashmakov, and E. G. Bessonov, *Zh. Tekh. Fiz.* **42**, 1921 (1972) [*Sov. Phys. Tech. Phys.* **17**, 1540 (1972/3)]; *Trudy FIAN SSSR* **80**, 100 (1975) [Proceedings of the Lebedev Institute].

<sup>20</sup>V. N. Baier, V. M. Katkov, and V. M. Strakhovenko, *Zh. Eksp. Teor. Fiz.* **63**, 2121 (1972) [*Sov. Phys. JETP* **36**, 1120 (1973)].

<sup>21</sup>K. Codling and R. Madden, *J. Appl. Phys.* **36**, 380 (1965).

<sup>22</sup>R. Haensel and C. Kunz, *Z. Angew. Phys.* **23**, 276 (1967).

<sup>23</sup>B. N. Meleshkin, V. V. Mikhaïlin, *et al.*, *Trudy FIAN SSSR* **80**, 140 (1975) [Proceedings of the Lebedev Institute].

<sup>24</sup>E. M. Rowe and F. E. Mills, *Particle Accelerators* **4**, 211 (1973).

<sup>25</sup>T. D. Mokul'skaya, M. A. Mokul'skii, A. A. Nikitin, A. N. Skrinskii, V. V. Anashin, G. N. Kulipanov, and V. A. Lukashev, *Dokl. Akad. Nauk SSSR* **218**, 824 (1974) [*Sov. Phys. Dokl.* **19**, 698 (1975)].

<sup>26</sup>H. Winick, cited in Ref. 16b, p. 685.

<sup>27</sup>P. Dagneaux *et al.*, *Ann. de Phys.* **9**, 65 (1975).

<sup>28</sup>E. S. Gluskin, V. A. Kochubei, A. A. Krasnoperova, L. N. Mazalov, S. I. Mishnev, A. N. Skrinskii, E. M. Trakhtenberg, and G. N. Tumaikin, *Izv. AN SSSR, Ser. Fiz.* **40**, 227 (1976) [*Bull. USSR Acad. Sci., Phys. Ser.*].

<sup>29</sup>A. N. Skrinskii, in: *Trudy V Vsesoyuznogo soveshchaniya po uskoritelyam zaryazhennykh chastits (Proceedings of the Fifth All-Union Conference on Charged-Particle Accelerators)*. Moscow, Nauka, 1977.

<sup>30</sup>E. Koch, C. Kunz, and E. Wiener, *The New Synchrotron Radiation Laboratory at the DESY Storage Ring DORIS, DESY SR-76/02* (1976).

<sup>31</sup>M. Sands, *The Physics of Electron Storage Rings*, SLAC Report No. 121 (1970).

<sup>32</sup>S. E. Baru, T. D. Mokul'skaya, M. A. Mokul'skii, V. A. Sidorov, and A. G. Khabakhpashev, *Dokl. Akad. Nauk SSSR* **227**, 82 (1976) [*Sov. Phys. Dokl.* **21**, 157 (1975)].

<sup>33</sup>G. N. Kulipanov, N. A. Mezentsev, I. Ya. Protopopov, V. B. Khlestov, V. S. Shabanov, and M. A. Sheromov, in: *Turdy I Vsesoyuznogo soveshchaniya po avtomatizatsii nauchnykh issledovaniy v yadernoi fizike (Proceedings of the First All-Union Conf. on Automation in Nuclear Physics Research)*, Kiev, 1976, p. 110.

<sup>34</sup>V. P. Koronkevich, G. N. Kulipanov, V. I. Nalivaiko, V. F. Pindur, and A. N. Skrinskii, *Kontaktnoe proetsirovanie mikroob'ektorov rentgenovskim sinkhrotronnym izlucheniem (Contact Projection of Micro-objects by X-Ray Synchrotron Radiation)*, Preprint 77-10, Nuclear Physics Institute, Novosibirsk, 1977.

<sup>35</sup>M. Hart, *J. Appl. Crystallogr.* **8**, 436 (1975).

<sup>36</sup>Z. G. Pinsker, *Dinamicheskoe rasseyaniye rentgenovskikh luchej v ideal'nykh kristallakh (Dynamic Scattering of X Rays in Ideal Crystals)*, Moscow, Nauka, 1974.

<sup>37</sup>P. Horowitz and J. A. Howell, *Science* **178**, 608 (1972).

<sup>38</sup>A. M. Kondratenko and A. N. Skrinskii, *Ispol'zovanie izlucheniya élektronnykh nakopitelei v rentgenovskoi golografiy mikroob'ektorov (Use of Radiation from Electron Storage Rings in X-Ray Holography of Micro-objects)*, Preprint 75-102, Nuclear Physics Institute, Novosibirsk, 1975.

<sup>39</sup>A. M. Kondratenko and A. N. Skrinskii, *Rentgenovskaya golografiya mikroob'ektorov (X-Ray Holography of Micro-objects)*, Preprint 76-105, Nuclear Physics Institute, Novosibirsk, 1976.

<sup>40</sup>G. W. Stroke, *Introduction to Coherent Optics and Holography*, Academic Press. Russ. transl., Moscow, Mir, 1967.

<sup>41</sup>A. A. Vazima, in: *Molekulyarnaya biologiya (Molecular Biology)*, No. 8, Moscow, VINITI, 1976, p. 86.

<sup>42</sup>A. Herzenberg and H. Lau, *Acta Crystallogr.* **22**, 24 (1967).

<sup>43</sup>S. E. Baru, G. N. Kulipanov, T. D. Mokul'skaya, M. A. Mokul'skii, A. A. Nikitin, V. A. Sidorov, A. N. Skrinskii, I. Ya. Skuratovskii, and A. G. Khabakhpashev, *Kristallografiya* **22**, 422 (1977) [*Sov. Phys. Crystallogr.* **22**, (1977) (in press)].

<sup>44</sup>V. A. Bryzgunov, *Prib. Tekh. Eksp.*, No. 6, 188 (1968) [*Instrum. Exper. Tech.*].

<sup>45</sup>F. W. Lytle, D. E. Sayers, and E. A. Stern, *Phys. Rev.* **B11**, 4825 (1975).

<sup>46</sup>A. A. Krasnoperova, E. S. Gluskin, and L. N. Mazalov, *Zh. Strukt. Khim.* **17**, 1113 (1976) [*J. Struct. Chem. (USSR)*].

<sup>47</sup>G. V. Gadiyak, D. A. Kirzhnits, and Yu. E. Lozovik, *Zh. Eksp. Teor. Fiz.* **69**, 122 (1975) [*Sov. Phys. JETP* **42**, 62 (1975)].

- <sup>48</sup>I. A. Ovsyannikova, S. B. Ėrenburg, V. B. Khlestov, I. I. Geguzin, I. A. Topol', V. P. Sachenko, and A. P. Kovtun, *Izv. AN SSSR, Ser. Fiz.* **40**, 230 (1976) [*Bull. USSR Acad. Sci., Phys. Ser.*].
- <sup>49</sup>K. Ishii, S. Morita, H. Tawara, T. Chu, H. Kaji, and T. Shiokawa, *Nucl. Instrum. and Meth.* **126**, 75 (1975).
- <sup>50</sup>V. A. Il'in, G. M. Kazakevich, G. N. Kulipanov, L. N. Mazalov, A. M. Matyushin, A. N. Skrinskiĭ, and M. A. Shermooov, *Rentgenofluorestsentyii ėlementnyii analiz s ispol'zovaniem sinkhrotronnogo izlucheniya (X-Ray Fluorescence Chemical Analysis with Synchrotron Radiation)*, Preprint 77-13, Nuclear Physics Institute, Novosibirsk, 1977.
- <sup>51</sup>V. F. Dmitriev and Ė. V. Shuryak, *Zh. Eksp. Teor. Fiz.* **67**, 494 (1970) [*Sov. Phys. JETP* **40**, 244 (1971)].
- <sup>52</sup>C. Sparks, J. Raman, *et al.*, *Phys. Rev. Lett.* **38**, 205 (1977)
- <sup>53</sup>A. N. Artem'ev *et al.*, *Zh. Eksp. Teor. Fiz.* **64**, 261 (1973) [*Sov. Phys. JETP* **37**, 136 (1973)].
- <sup>54</sup>A. M. Afanas'ev and Yu. Kagan, *Zh Eksp. Theor. Fiz.* **48**, 327 (1965) [*Sov. Phys. JETP* **21**, 215 (1965)].
- <sup>55</sup>V. N. Korchuganov, G. N. Kulipanov, N. A. Mezentsev, V. F. Pindyurin, A. N. Skrinskiĭ, M. A. Sheromov, and V. B. Khlestov, *Metod operativnogo izmereniya absolyutnoi energii chastits v nakopitele s ispol'zovaniem spektral'nykh osobennostei sinkhrotronnogo izlucheniya (Method of Operative Measurement of the Absolute Energy of Particles in a Storage Ring with Use of the Spectral Features of Synchrotron Radiation)*, Preprint 77-9, Nuclear Physics Institute, Novosibirsk, 1977.
- <sup>56</sup>E. Spiller, D. Eastman, R. Feder, W. Crobman, W. Gudat, and J. Topalian, *Application of Synchrotron Radiation to X-Ray Lithography*, DESY SR 76/11 (1976).
- <sup>57</sup>J. W. McGowan, Private communication.
- <sup>58</sup>S. N. Ivanov, G. N. Kulipanov, I. N. Luchnik, V. V. Mikhailin, V. B. Khlestov, and A. V. Khudyakov, *Izv. AN SSSR, Ser. Fiz.* **41**, 352 (1977) [*Bull. USSR Acad. Sci., Phys. Ser.*].

Translated by Clark S. Robinson

## The non-self-sustaining gas discharge for exciting continuous-wave gas lasers

E. P. Velikhov, V. D. Pis'mennyĭ, and A. T. Rakhimov

*I. V. Kurchatov Institute of Atomic Energy  
and Nuclear Physics Institute of the Moscow State University  
Usp. Fiz. Nauk* **122**, 419-447 (July 1977)

This review devotes its major attention to analyzing the physical processes that govern the stability of uniform burning of the volume gas discharges that are used to excite high-pressure CO<sub>2</sub> lasers. An analysis is given of the theoretical and experimental studies that have shown a substantial increase in the time of uniform burning of a non-self-sustaining gas discharge as the electric power density is decreased. Specifically, this has made it possible to convert the discharge in practice into a steady-state burning regime at elevated gas pressure. The optical characteristics of gas mixtures based on carbon dioxide that are established upon excitation of the medium by a steady-state non-self-sustaining discharge are examined.

PACS numbers: 51.50.+v, 42.55.Dk

### CONTENTS

1. Introduction . . . . .	586
2. The Uniform Self-Sustaining Glow Discharge in Gases at Elevated Pressure . . . . .	588
3. Burning and Stability of the Non-Self-Sustaining Gas Glow Discharge . . . . .	592
4. Optical Characteristics of Gaseous Media Based on CO <sub>2</sub> when excited by a Steady-State Non-Self-Sustaining Discharge . . . . .	600
5. Conclusion . . . . .	601
Bibliography . . . . .	601

### 1. INTRODUCTION

The interest in CO<sub>2</sub> lasers that operate at elevated pressures of the working medium (of the order of a hundred torr and higher), and which are excited by a non-self-sustaining gas discharge, is explained by the possibility of attaining high energy densities and efficiencies of laser action in these systems.

The gas discharge as used for exciting CO<sub>2</sub> lasers is a glow discharge whose plasma is very weakly ionized: the fraction of charged particles with respect to the concentration of atoms and molecules is of the order of 10<sup>-6</sup>-10<sup>-8</sup>. The temperature of the electrons in the gas-discharge plasma as established by the action of the

electric field is about 1 eV, while the temperature of the gas is close to room temperature. The thermodynamic non-equilibrium of the plasma, which is specifically what creates the inverted population of the vibrational levels of the CO<sub>2</sub> molecules, is determined by the greater heat capacity of the gas than that of the charged particles. Yet the heating of the neutral particles that occurs during the burning of the discharge limits the duration of laser action in pulsed lasers. Heat is usually removed from the gas in continuous-wave lasers by pumping the gas through the discharge volume.

In a self-sustaining discharge, the electric field that is established in the discharge, and correspondingly,